





Updated concepts of seismic gaps and asperities to assess great earthquake hazard along South America

Thorne Lay^{a,1} and Stuart P. Nishenko^a

INAUGURAL ARTICLE

This contribution is part of the special series of Inaugural Articles by members of the National Academy of Sciences elected in 2014. Contributed by Thorne Lay, received October 2, 2022; accepted November 9, 2022; reviewed by Sergio Barrientos, Susan Beck, and Lynn R. Sykes

So far in this century, six very large-magnitude earthquakes $(M_W \ge 7.8)$ have ruptured separate portions of the subduction zone plate boundary of western South America along Ecuador, Peru, and Chile. Each source region had last experienced a very large earthquake from 74 to 261 y earlier. This history led to their designation in advance as seismic gaps with potential to host future large earthquakes. Deployments of geodetic and seismic monitoring instruments in several of the seismic gaps enhanced resolution of the subsequent faulting processes, revealing preevent patterns of geodetic slip deficit accumulation and heterogeneous coseismic slip on the megathrust fault. Localized regions of large slip, or asperities, appear to have influenced variability in how each source region ruptured relative to prior events, as repeated ruptures have had similar, but not identical slip distributions. We consider updated perspectives of seismic gaps, asperities, and geodetic locking to assess current very large earthquake hazard along the South American subduction zone, noting regions of particular concern in northern Ecuador and Colombia (1958/1906 rupture zone), southeastern Peru (southeasternmost 1868 rupture zone), north Chile (1877 rupture zone), and north-central Chile (1922 rupture zone) that have large geodetic slip deficit measurements and long intervals (from 64 to 154 y) since prior large events have struck those regions. Expanded geophysical measurements onshore and offshore in these seismic gaps may provide critical information about the strain cycle and fault stress buildup late in the seismic cycle in advance of the future great earthquakes that will eventually strike each region.

asperities | seismic gaps | slip deficit | South American large earthquakes | seismic hazards

Earth's largest earthquakes occur on subduction zone plate boundary faults, or megathrusts, where stick-slip sliding accommodates convergent relative plate motions. Long-term relative plate motions result in episodic stress buildup and elastic strain accumulation on either side of frictionally locked portions of the megathrusts followed by abrupt fault sliding offsets and surrounding strain energy release in large earthquakes as the system strives to keep up with the long-term relative plate motions. The underlying conceptual framework dates back to the elastic-rebound theory that emerged from the 1910 work of Reid (1) following the 1906 San Francisco earthquake and the recognition of large-scale plate tectonics in the 1960s. Uncertainties in stress drop relative to absolute stress levels, variability in failure stress level, fluctuations in fluid pressure distributions, nonlinear frictional instabilities, complexity of megathrust physical properties, and adjacent earthquake stress interactions (2) result in space and time irregularities of very large megathrust earthquake occurrence. Nonetheless, as earthquake observations continue to accumulate, there has been substantial progress in understanding megathrust earthquake hazard in the context of the tectonic strain energy budget for the system; the so-called Reid renewal interval of strain reaccumulation that must occur before another very large earthquake ruptures a given portion of the plate boundary.

The focus here is on the subduction zone extending ~6,500 km along the western coast of South America, where the Nazca plate is underthrusting the South American plate. The occurrence of 6 very large megathrust earthquakes ($M_W > 7.8$) along this plate boundary during the last 21 y (Fig. 1) has reinforced several fundamental observations that were made about great earthquake occurrence more than 50 y ago:

- The rupture zones of major earthquakes along geometrically simple megathrusts tend to abut without significant overlap.
- Very large earthquakes ($M_W \ge 7.8$) have a tendency to occur along portions of the megathrust where comparable size earthquakes have not occurred for many decades or even several centuries (3, 4). These regions are called seismic gaps.

Significance

Earthquakes involve complex, nonlinear frictional instabilities and dynamical processes that undermine deterministic predictability. Nonetheless, plate boundary strain energy budgets, driven by long-term relative plate motions, provide a degree of cyclicity in occurrence of very large earthquake ruptures on subduction zone plate boundary (megathrust) faults. For the largest earthquakes, a basic cycle of interseismic fault locking and strain accumulation, abrupt coseismic fault sliding and strain energy release, and postseismic stress adjustment occurs, basically compatible with the elastic-rebound theory of faulting. Heterogeneous slip and triggering interactions give rise to irregularity in this seismic cycle, but by quantitatively characterizing the slip in very large earthquakes in regions that have previously ruptured in large historic earthquakes, improved understanding of future earthquake hazards is possible.

Author contributions: T.L. and S.P.N. designed research; performed research; and wrote the paper.

Reviewers: S. Barrientos, National Seismological Center, Univ. of Chile; S. Beck, University Arizona; and L.R.S., Columbia University.

The authors declare no competing interest.

Copyright © 2022 the Author(s). Published by PNAS. This open access article is distributed under Creative Commons Attribution License 4.0 (CC BY).

¹To whom correspondence may be addressed. Email:

This article contains supporting information online at https://www.pnas.org/lookup/suppl/doi:10.1073/pnas. 2216843119/-/DCSupplemental.

Published December 13, 2022.

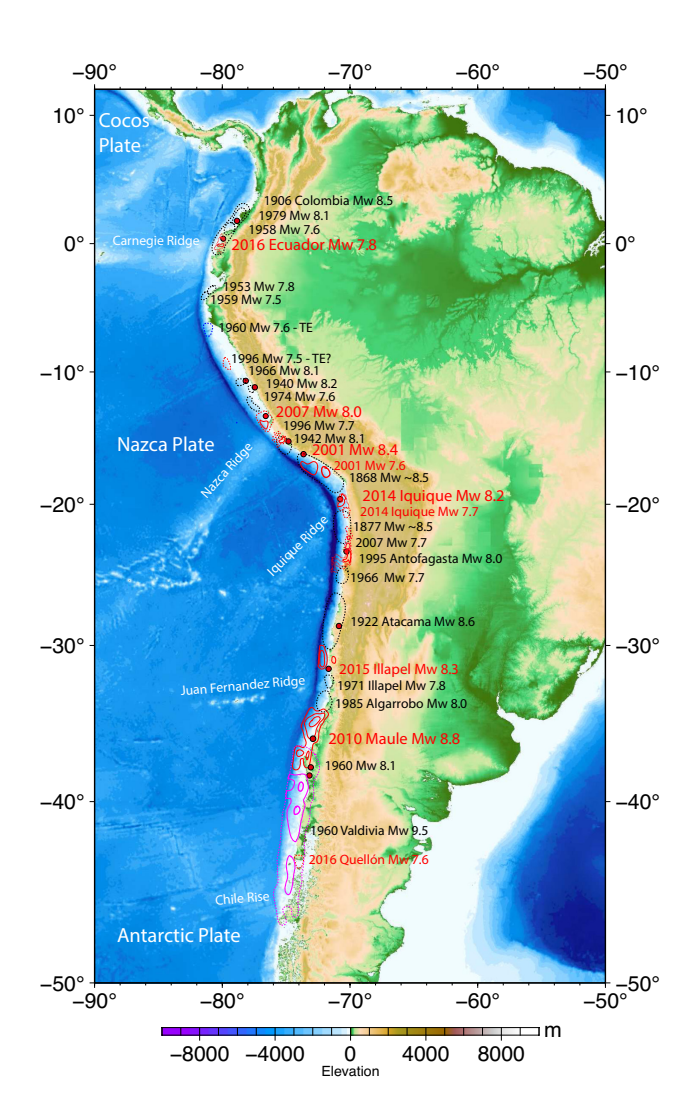


Fig. 1. The most recent large earthquake rupture zones ($M_W \ge 7.5$) along each region of the west coast of South America where the Nazca plate is underthrusting the continent. Black dashed regions indicate aftershock zones for older events (black labels); red contours indicate slip distribution for large events in this century (red labels) from references in the supplement; purple contours indicated slip contours (1, 10, and 20 m) for the 1960 Valdivia, Chile, event

The first point is readily evident in the nearly continuous distribution of the most recent large earthquake rupture zones along the entire boundary depicted in Fig. 1. The large events since 2000 are shown with coseismic slip contours that emphasize the nonuniform slip along dip and along strike of the subduction zone. Most of the Nazca-South America plate boundary has produced repeated large earthquakes along the full distribution of ruptures shown in Fig. 1. The second point above is demonstrated by considering the estimated along-strike extent of large historic earthquakes $(M_W \ge -7.5)$ along the South American subduction zone shown in Fig. 2. It is important to note that there are examples where recent very large earthquakes have ruptured smaller areas than in prior events (this is notable for the 2016 Ecuador earthquake (Fig. 2A), which reruptured the 1942 zone but only ruptured the southern portion of the 1906 zone, and the 2001 southern Peru event (Fig. 2B), which ruptured about 2/3 of the length of the 1868 event, as well as examples where earthquakes have ruptured areas larger than in prior events (the 2010 Maule, Chile, earthquake (Fig. 2C) ruptured the 1928 zone plus most of the 1835 zone). One has to be cautious about inferring overlap of two-dimensional ruptures, as for the case of the 2007 northern

Chile rupture, located on the down-dip portion of the megathrust, which may not overlap shallow rupture in the 1877 event (5). Nonetheless, it is clear that absolute segmentation does not exist, and ruptures can comprise multiple adjacent portions of the boundary or not, an aspect that was not well recognized in the early seismic gap discussions.

About 43 y ago, an additional key concept involving slip heterogeneity in megathrust earthquakes developed from observations of variations in maximum earthquake size and complexity of seismic waves radiated from very large earthquakes in different subduction zones. Regions on the fault with large coseismic slip and associated large volumetric strain release are identified as "asperities," borrowing a contact mechanics term for the point contacts of microscale surface interactions (10-12). Patchy distributions of large-slip regions during large earthquakes have been affirmed by increasingly well-resolved finite-fault slip models, but whether the underlying cause is material property variations (sediments/rock contacts), boundary roughness (seamounts/horst and graben structures), or hydrologic variations (pore fluids), or some combination of these factors, and their persistence over multiple events is still an active area of research. A somewhat complementary perspective of earthquake ruptures being controlled by portions of the fault that delimit sliding, or "barriers," was also advanced about this time (13). The connection between asperities, barriers, and gaps is intrinsically complex as heterogeneity of stress and strain accumulation and variable frictional properties complicate the notion of a fault "sticking," which is intrinsic to the elastic-rebound theory (14). While some faults may actually lock up uniformly over their entire seismogenic surface and rupture accordingly, others may have patchy locking and irregular failure with mixed seismic and aseismic modes of boundary sliding, leading to distributions of event size on the same megathrust, partial rupture within a seismic gap, and variability in great earthquake size in a given region.

While the early conceptual models of seismic gaps and asperities have guided many analyses of large earthquakes over the past decades, major advances over the past 30 y in understanding the complexity of frictional behavior, development of geodetic methods for directly detecting interseismic strain accumulation in the upper plate of subduction zones, and joint seismic—geodetic—tsunami analyses of finite-fault slip distributions have provided a more physical context for understanding heterogeneity of slip on faults. The inferred "patchiness" of megathrust geodetic locking and large event slip irregularity give a better understanding of why large event ruptures tend not to overlap with recent events and why some events can rupture regions that at other times fail in several discrete events. Stress shadowing along dip and along strike can result in slip deficit before and after large events in regions that are not mechanically coupled (15).

We draw on the updated perspectives of seismic gaps, persistent asperities, and geodetic locking to evaluate the current state of seismic hazard for very large earthquakes along the Nazca–South American megathrust. Our focus is on very large event hazards $(M_W \ge 7.8)$. These very large events release the majority of accumulated tectonic strain over large enough portions of the plate boundary (-120 km × 40 km) for Reid renewal models to be applicable. Smaller ruptures can have adjacent rupture patches that may not involve rerupture of a common megathrust region making them more ambiguous to interpret. The identification of seismic gaps for very large events along the South American subduction zone in the 1970s (16) helped to focus earthquake research and monitoring activities during the following decades. While efforts to assess the relative probability of major ruptures in identified seismic gaps became controversial (17–23), being

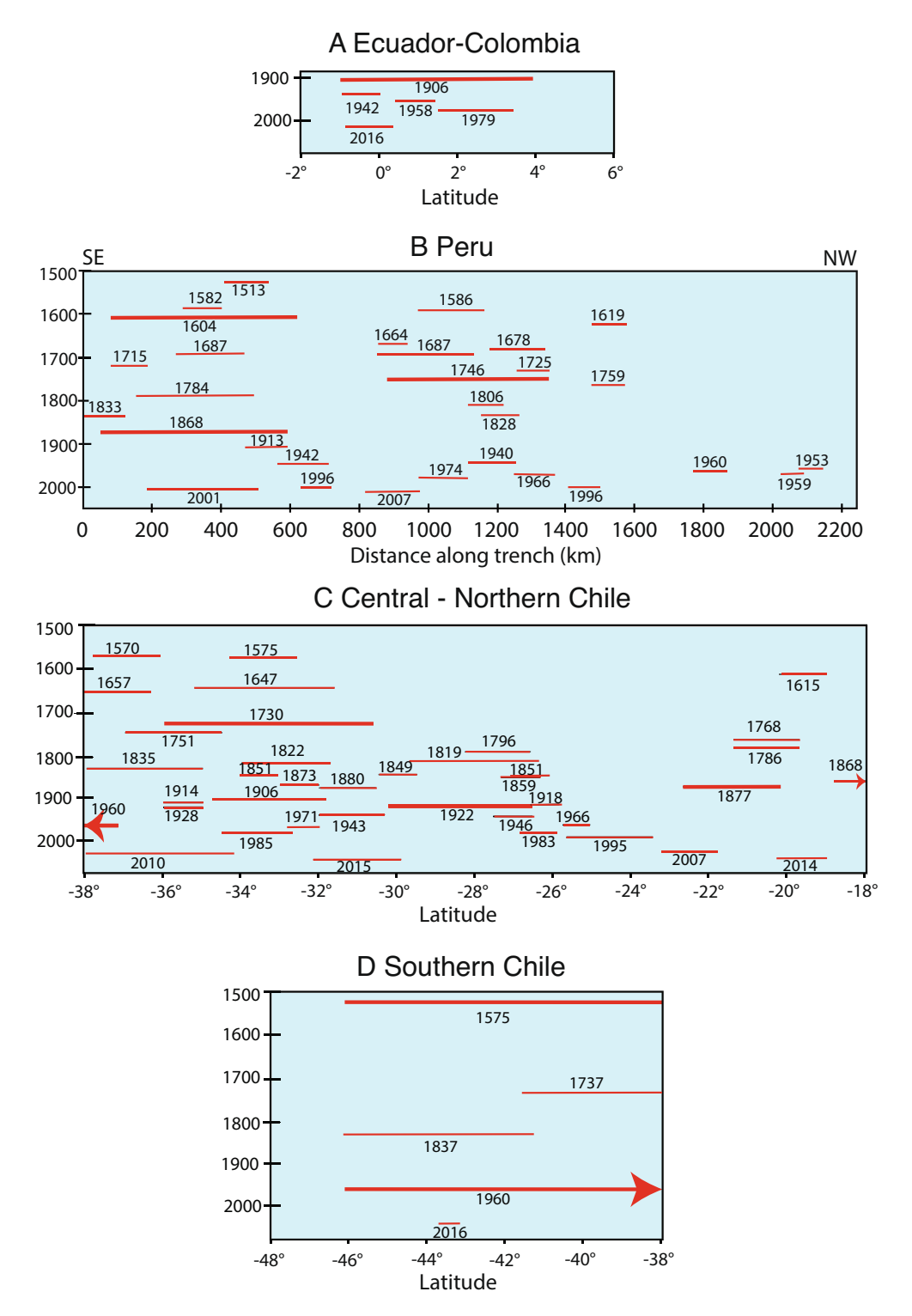


Fig. 2. Along-plate boundary rupture distributions for historic large earthquakes ($M \ge \sim 7.5$) in (A) Ecuador–Colombia, (B) Peru (6), (C) central to northern Chile (7–9), and (D) southern Chile (7, 8). Bolder lines represent Breakthrough Ruptures that likely span the entire width of the plate boundary.

handicapped by consideration of smaller events and the limited information about very large historic earthquakes, almost all very large megathrust earthquakes during the past 50 y have, in fact, been located along subduction zone segments where multiple-decade intervals of prior strain accumulation had occurred (24). Only a handful of recent very large earthquakes have ruptured localized areas where a previous comparable or much larger earthquake was seismically observed, so quantitative comparisons of successive dynamic ruptures remain very limited.

Deployment of geodetic and seismic monitoring instruments in many of the early identified seismic gaps throughout the circum-Pacific region has enhanced the resolution of subsequent faulting processes, revealing heterogeneous coseismic slip on the megathrust fault. New technologies, including global and regional broadband seismograph networks, space-based geodesy (GNSS), satellite interferometry (InSAR), seafloor geodesy (GNSS-a, ocean bottom pressure sensors), seafloor drill hole facilities, and potential field (gravity) measurements, have dramatically improved the ability to quantify

long-term strain accumulation and relaxation, as well as short-term coseismic processes, along plate boundaries.

Results

The following sections consider the fundamental observations concerning the abutting of rupture zones and time-dependent recurrence behavior along the South American plate boundary in the light of recent great earthquakes and the 50 y of subsequent research advances since the initial seismic gap and asperity papers were published. We discuss the spatial and temporal patterns of great earthquake ruptures in the context of updated physical models of the megathrust and identify segments of the plate boundary that appear to have elevated seismic hazard of very large earthquakes within the coming decades. Improved understanding of very large earthquakes on plate boundaries is emerging from observations of many global events (24), but key insights can be captured from consideration of the six recent events along the South American subduction zone. Major observations and lessons learned from these events are summarized below. Detailed discussion and citations for each event are presented in the Supplement.

2016 Ecuador. The 16 April 2016 M_W 7.8 Pedernales, Ecuador, earthquake (Figs. 1, 2A, and 3A) ruptured the down-dip portion of the Colombia/Ecuador seismogenic zone along prior ruptures in 1906 (M_W 8.6) and 1942 (M_W 7.8). Large events to the northeast in 1958 and 1979 fill in most of the 1906 rupture length, demonstrating that great ruptures can intermingle with multiple shorter but still very large events (25). The source region had previously been accumulating moderate slip deficit based on geodetic measurements (26). Comparison of seismic waveforms and magnitudes demonstrate that the 2016 and 1942 events have similar surface wave magnitudes $(M_s 7.5)$, overlapping rupture areas, and an overlapping large-slip patch (Fig. 3A) but not identical teleseismic waveforms—indicating that 2016 was a quasirepeat of 1942 (27). This is further discussed in the Supplement. A distribution of slip-weakening patches along strike appears to be characteristic of this region.

2007 Pisco, Peru. The 15 August 2007 (M_W 8.0) Pisco, Peru, earthquake produced substantial shaking damage and a large tsunami on the southern Paracas Peninsula (Figs. 1, 2B, and

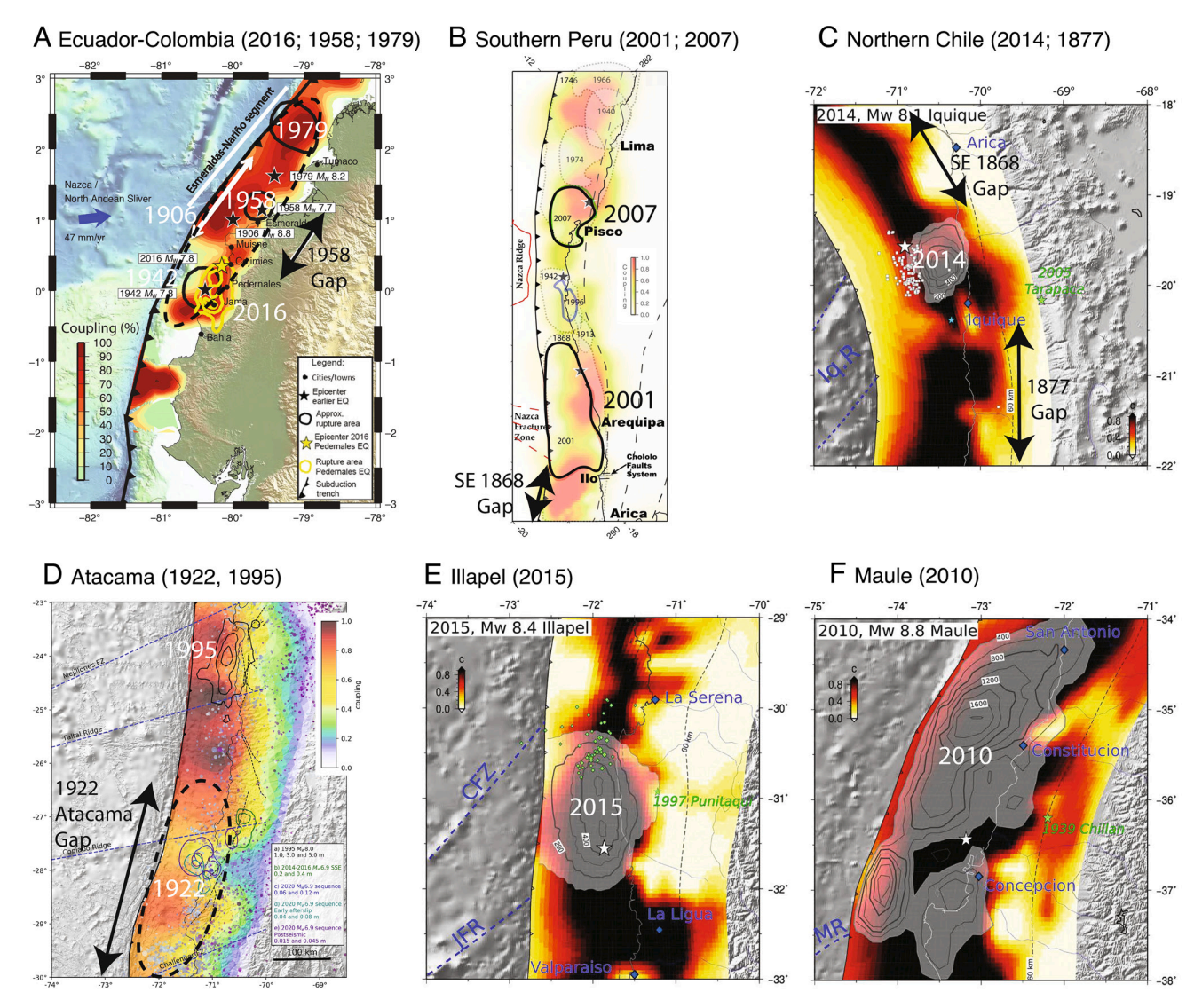


Fig. 3. Very large earthquake rupture zone and prior estimates of geodetic plate boundary coupling (darkest reds correspond to 100% slip deficit relative to plate motion) for (*A*) the 2016 Ecuador earthquake and 1906, 1942, 1958, and 1979 ruptures (28); (*B*) the Southern Peru region with the 2007 Pisco and 2001 Arequipa earthquakes (29); (*C*) the 2014 Iquique, Chile, zone, with 1868 Peru to the north and 1877 Chile to the south (9); (*D*) the 1922 Atacama event region with the 1995 Antofagasta earthquake to the north (30); (*E*) the 2015 Illapel earthquake (9); and (*F*) the 2010 Maule, Chile, earthquake (9).

3B). The event is among a sequence of great earthquakes in Central Peru that progressively reruptured the larger 1687 and 1746 zones (Fig. 2B) in 1940 $(M_W \hat{8}.2)$, 1942 $(M_W \hat{8}.1)$, 1966 $(M_W 8.1)$, 1974 $(M_W 7.6)$, and 2007 $(M_W 8.0)$ (31). Geodetic slip deficit had been observed prior to the 2007 rupture (29). The seismic, geodetic, and tsunami data for this event reveal that the rupture involved two or more large-slip patches straddling the peninsula with about a 60-s lag time between the primary subevents (32). The discrete triggering of separated large-slip patches and adjacent up-dip and along-strike afterslip (33) are consistent with the asperity model.

2001 Southern Peru. The 23 June 2001 M_W 8.4 Arequipa (or Camaná), Peru, earthquake and its magnitude 7.6 aftershock on 7 July 2001 to the southeast reruptured the northern twothirds of the 1868 seismic gap (Figs. 1, 2B, and 3B). Earthquake intensity and tsunami run-up reports indicate that great events in 1604 and 1868 were larger than those in the overlapping 1582, 1784, and 2001 earthquakes (Fig. 2B) (31,34). Based on analysis of seismic, geodetic, and tsunami data, the earthquake broke two spatially offset asperities: the first in the northwest of the rupture zone and the second, centrally located asperity being much larger and releasing most of the total seismic moment (29, 32, 35). Rupture appears to have extended across the megathrust to near the trench.

2014 Iquique, Chile. The 1 April 2014 M_W 8.1 Iquique, Chile, earthquake and its large M_W 7.7 aftershock on 3 April 2014 to the south ruptured a rather compact area of the northern Chile central megathrust from 19.3°S to 20.7°S (Figs. 1, 2C, and 3C). The rupture was preceded by months of slowly migrating foreshock activity located up-dip of the eventual mainshock, indicating along-dip variation in frictional properties of the megathrust (36, 37). The large-slip zone (-2 to 7 m) for the 2014 mainshock extends only about 70 km along strike and 50 km along dip, with finite-slip models being well resolved by seismic, geodetic, and tsunami observations (38, 39). The concentrated mainshock slip, with adjacent down-dip slow deformation and afterslip, is consistent with the asperity model, and several prior historical earthquakes have occurred in this region of northernmost Chile over the past few centuries (Fig. 2C), so persistence of localized velocity-weakening properties is viable. The event struck in an area of large slip deficit inferred from geodesy that extends along northern Chile from 18°S to 25°S, with a low-coupling zone near 21°S (40). Many estimates of the 1877 rupture extent span this region (41, 42), so early interpretations viewed the 2014 event as a partial rupture of the 1877 zone akin to the events along Ecuador-Colombia. However, based on detailed reinterpretation of intensity observations for 1877, the 2014 Iquique event appears to have ruptured within the megathrust region south of Arica and north of Iquique that lies between large-slip regions of the great 1868 Peru and 1877 Chile earthquakes (43) (Fig. 3C).

2015 Illapel, Chile. The 16 September 2015 M_W 8.3 Illapel, Chile, earthquake ruptured ~170 km along the plate boundary megathrust in central Chile from 30°S to 31.8°S (Figs. 1 and 3*E*). This event struck in the same region as events in 1943, 1880, and 1730 (Figs. 2*C* and 3*E*) (18, 44). The 2015 Illapel earthquake is of particular note because rapid seismic magnitude estimation of the event prompted a tsunami warning and evacuation notifications within 8 to 11 min of the origin time, resulting in large-scale evacuation along the Chile coast (45). Seismic, geodetic, and tsunami waveform analyses of the 2015 Illapel earthquake indicate

concentrations of ~3-m coseismic slip below the coast and a large patch with up to ~10-m slip at shallow depths (46-48). Studies with the best offshore resolution are consistent with the largeslip patch having extended up-dip to near the trench. Geodetic measurements prior to the event indicate that there was strong megathrust coupling in the region of large slip, particularly south of 31°S, although resolution of coupling out to the trench is very low (49, 50), and afterslip expanded both northward and southward from the large-slip zone (51). The prior 1943 $M_W 7.9$ event has a single pulse of moment release at depths <35 km but has a smaller seismic moment estimate and simpler waveforms that indicate that it did not rupture the shallow portion of the megathrust (50). Local and far-field tsunami heights for the 2015 event are significantly higher than those in 1943. Overall, the 2015 event is not a simple repeat of the 1943 event and likely had much more slip at shallow depth (45).

2010 Maule, Chile. The 27 February 2010 Maule (M_W 8.8) earthquake ruptured the plate boundary offshore of central Chile between 34°S and 38.5°S (Figs. 1–3F). The coseismic slip of this event has been determined by analysis of seismic, geodetic, and tsunami observations. Patchy coseismic slip is distributed over a region 460 km long and 100 km wide between the depths of 15 and 40 km. Two large-slip asperity regions are resolved along the megathrust: one extending from 34°S to 36°S (with up to 20-m slip) and the other from 37°S to 38°S (with up to 10-m slip). Joint inversions with accurately modeled tsunami observations find that the large-slip patches include slip of 5 to 8 m all the way to the trench (52, 53). Geodetic measurements had resolved accumulating slip deficit prior to the rupture along the entire rupture area, with moderate reduction near 35°S (54), but the patchy slip distribution only loosely conforms to the variable locking distribution (55). Afterslip extends along the length of the rupture primarily down-dip and between the two large coseismic slip patches (56). Conventional seismic gap ideas with strong segmentation do not characterize this region well, but the Reid strain renewal concept in conjunction with a distribution of persistent asperities along the megathrust reconciles the historical behavior.

Discussion

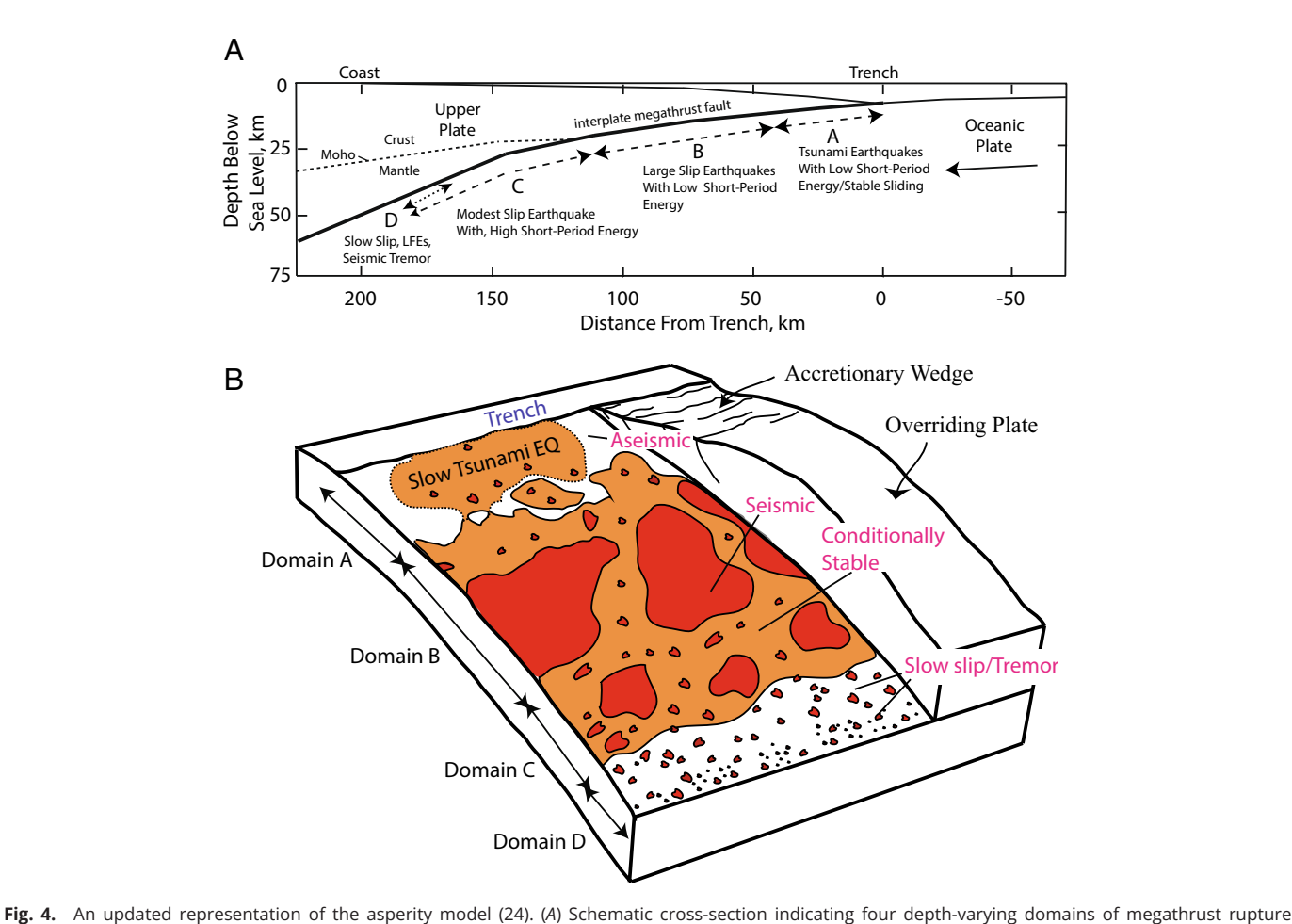
The quantification of interseismic, coseismic, and postseismic deformation for the six very large earthquakes along the South American subduction zone in the past 21 y described above provides insight into updated conceptual/observational seismic gap and asperity models. The intuitive concept of strain accumulation and release in the Reid renewal cycle continues to underlie validity of the seismic gap idea for very large earthquake occurrence, but strict segmentation of the plate boundary is not defined by recent rupture zones. Early estimates of the lateral extent of large ruptures relied heavily on aftershock zones as well as MMI VIII damage and tsunami reports. Recent, well-documented earthquakes help to calibrate these older descriptions (7). Coseismic slip heterogeneity and nonuniform slip deficit accumulation from seismic and geodetic inversions continue to be well accounted for by the asperity model, but evaluating persistence of these regions of slip-weakening properties is complicated by repeated very large earthquakes having variable slip both along dip and along strike. Representations of the asperity model have progressively added complexity to reflect along-dip variations and complexity of individual sequences (Fig. 4) (24, 57–59), and such models have been invoked in many earthquake studies. Along-dip variations are now recognized as particularly important, with the megathrust shallower than 15 km

(Domain A) potentially having strain accumulation that results in tsunami earthquakes or enhances ruptures that initiate deeper. Between 15 and 35 km (Domain B), the megathrust has discrete slip-weakening patches that are patchy and surrounded by slip-strengthening zones; the larger patches fail in very large earthquakes and may cascade to produce great earthquakes that span longer stretches of the boundary. Domain C extends from 35 to 50 km and has reduced size asperities and increasing aseismic component, but damaging earthquakes can still result as they tend to be below the coast. This region also produces stronger short-period radiation during very large earthquakes.

Bathymetric features on the subducting plate, notably the Chile Rise, Challenger Fracture Zone, Juan Fernandez Ridge, Nazca Ridge, Medaña Fracture Zone, and Carnegie Ridge, appear to act as persistent barriers to rupture along South America, defining major megathrust segments (3, 60). Finer-scale segmentation is controlled by asperity distributions on the megathrust, but only a few examples (1942/2016 Ecuador and 1943/2015 Illapel) of repeated ruptures with seismic recordings are available to evaluate the persistence of asperities through the seismic cycle. Megathrust

ruptures that span the entire width of the plate interface (Domains A+B+C), termed "Breakthrough Ruptures" (61), are proposed to "reset" the seismic cycle and are distinct from those events confined to deeper portions of the interface (Domain B or C only). Along the South American plate boundary, one can identify multiple Breakthrough Ruptures, including the 1575 and 1960 S. Chile, 1730 Valparaíso, 1819/1922 Atacama, 1877 N. Chile, 1604/1868 S. Peru, 1746 Central Peru, and 1906 Colombia–Ecuador events. From two to four events have reruptured most of the same regions in smaller, nonoverlapping events, giving rise to the space–time irregularity evident in Fig. 2 but still allowing regions of significant strain accumulation and potential for future events to be identified.

If we view seismic gaps in areas with prior very large earthquakes and/or current day slip deficit accumulation as regions with patchy asperities that must accumulate sufficient stress and strain to fail, one can generally infer relative seismic hazard based on historical and geodetic observations. Essentially, the updated asperity representation shown in Fig. 4 captures the essence of the asperity, seismic gap, and



rig. 4. An apparet representation of the aspenty moder (24). (A) schematic cross-section mulcitary four depth-varying domains of megathrust typical characteristics: A – near-trench domain where tsunami earthquakes or anelastic deformation and stable sliding occur; B – central megathrust domain where large slip occurs with minor short-period seismic radiation; C – down-dip domain where moderate slip occurs with significant coherent short-period seismic radiation; D – transitional domain, only present in some areas, typically with a young subducting plate, where slow slip events, low-frequency earthquakes, and seismic tremor can occur. At yet greater depths, the megathrust slides stably or with episodic slow slip or plastic deformation that does not generate earthquakes. (B) Cutaway schematic characterization of the megathrust frictional environment related to Domains A, B, C, and D defined in (A). Regions of unstable frictional sliding (asperities) are red regions labeled "seismic." Regions of aseismic stable or episodic slow sliding are white regions labeled "aseismic." Orange areas are conditional stability regions, which displace aseismically except when accelerated by failure of adjacent seismic patches. Domain A is at shallow depth where low-rigidity sediments and pore fluids cause very slow rupture expansion even if large displacements occur in tsunami earthquakes. Domain B has large, relatively uniform regions of stable sliding that can have large slip but generate modest amounts of short-period radiation upon failure. Domain C has patchy, smaller-scale regions of stable sliding surrounded by conditionally stable areas. When these areas fail, coherent short-period radiation is produced. Small, isolated patches may behave as repeaters when quasistatic sliding of surrounding regions regularly load them to failure. Domain D is dominated by aseismic sliding, but many small unstable patches can rupture in seismic tremor when slow slip events occur.

frictional heterogeneity perspectives, with the behavior of the larger asperities being emphasized here. With the 2016 Ecuador, 2007 and 2001 Peru, and the 2010 Maule events all involving coseismic rupture of at least two large asperities, and the 2001 Peru and 2014 Iquique, Chile, events having very large aftershocks along strike, the patchy nature of the megathrust asperity distribution has been clearly manifested in the recent South American events. The relatively uniform but modulated geodetic coupling on the megathrust along the South America coastline, with patchy ruptures and afterslip distributions for the recent very large events, provides further support for this conceptual model. However, time predictability remains elusive given the experience that some events involve cascades of several asperities failing together to make a great earthquake, some events likely have incomplete stress release due to lateral buttressing by adjacent regions that do not fail, and shallow megathrust failures may or may not accompany deeper megathrust failures. The recent events demonstrate this full range of behavior. Anticipating the size and timing of future events is thus highly uncertain, but as for the recent events, one can generally anticipate where large events are likely to occur.

With these perspectives in mind, we identify four regions of particular interest for future large earthquake occurrence.

Ecuador/Colombia: Esmeraldas (~1°N)

The region just north of the 2016 M_W 7.8 Ecuador rupture (Figs. 1, 2A, and 3A) last ruptured with a comparable size event in 1958 (M_W 7.6). Viewing the deeper megathrust region as having several large asperities distributed along strike, the 2016 failure has increased driving stress on the 1958 zone, which already has 64 y of possible strain accumulation, exceeding that between the 1906 and 1958 events. Aftershock activity for the 2016 event has concentrated offshore and along the southwestern portion of the 1958 zone. Localized strong geodetic coupling in the 1958 rupture zone adds to the earthquake potential in this region.

Southeasternmost Peru: Arica (~18 to 19°S)

The 1604 and 1868 MMI VIII isoseismal zones both extend farther southeast toward Arica, Chile, than the 2001 rupture (Figs. 1, 2B, and 3B), indicating that the southeasternmost portion of the Peru plate boundary has remained unbroken for 154 y (34, 62). Geodetic slip deficit accumulation in the area is high (~63 mm/y) indicating that as much as ~10 m of slip may have accumulated in the region since 1868, with potential seismic moment equivalent to an M_W 8.4 event. It is unclear why the 2001 event failed to rupture into this region, but there is evidence for prior smaller events that ruptured just this region in 1833 and 1715 (Fig. 2B).

Northern Chile: Loa (~21 to 23°S)

The Loa segment between Iquique and Antofagasta corresponds to the large-slip region of the great 1877 Arica earthquake based on intensity reports (41, 43) and is bounded to the north by the $2014 M_W 8.2$ Iquique earthquake and to the south by the 1995 M_W 8.0 Antofagasta rupture (Figs. 1, 2C, and 3C). The Loa segment exhibits high geodetic coupling along its entire length (Fig. 3C), and the area between 20° and 21°S has had little to no seismic activity during the last century (39). The rate of slip deficit accumulation in the area (~55 mm/y) (63) indicates that as much as ~8 m of slip has accumulated in the region since 1877, with potential seismic moment equivalent to an $M_W 8.4$ event. Rupture of the shallow megathrust up-dip of the 2007 rupture zone as part of this event is viable.

Northern Chile: Vallenar/Atacama (~26 to 29.5°S)

This region last ruptured in the great M_w 8.6 Atacama earthquake of 10 November 1922 and is bounded to the north by the 1995 $M_{\rm W}$ 8.0 Antofagasta rupture and to the south by the 2015 Illapel $M_W 8.3$ earthquake (Figs. 1, 2C, and 3D). The northern region of the 1922 rupture zone, from 26°S to 27°S, has experienced relatively frequent large ruptures, in 1796 (M ~ 7.5), 1819 (M ~ 8.5), 1859 (M ~ 7.5), 1918 (M ~ 7 to 7.5), 1922, 1946, and 1983 (M_W 7.6), while the southern region from 27°S to 29.5°S appears to have ruptured only in 1819 and 1922 (7,8,64) (Fig. 2C). The 1922 event likely exhibited bilateral rupture (65) and a complex slip distribution involving the rupture of three separate asperities, seemingly consistent with eyewitness accounts (44). The prior rupture in 1819 involved a sequence of three events on April 3, 4, and 11 (8). The very large earthquake pairs in 1796/1819 and 1918/1922 have been suggested to represent the primary plate boundary ruptures for the Vallenar/Atacama segment, indicating a repeat time for this segment of the Chilean subduction zones of on the order of a century. Geodetic surveys provide a clear mapping of heterogeneous interseismic coupling along the 1922 rupture zone with high coupling at both shallow (8 to 15 km) and intermediate (15 to 35 km) depths (30, 49, 63) (Fig. 3D). The southern boundary of the 1922 rupture, near La Serena (30°S), is coincident with the intersection of the Challenger Fracture Zone, and the local low geodetic coupling is proposed to act as a persistent barrier between great earthquake rupture in the Atacama and south-central Chile segments (66). For an estimated slip deficit rate of ~50 mm/y (63), ~5 m of slip may have accumulated during the last 100 y comparable with an M_W 8.3 earthquake.

Looking forward, sustained operation or new deployment of dense networks of seismic, onshore and offshore geodetic, and tsunami sensors is essential to making sufficient observations of the deformation process in these four regions that will inevitably culminate in future very large earthquakes. Large-scale space-time patterns of regional seismicity may help to identify regions approaching their limiting strain accumulation (61, 67). Of course, large events can also occur in regions where strain accumulation is thought to be modest; the 2016 M_W 7.6 earthquake in the 1960 rupture zone (Fig. 2D) is one such example. Imprecise knowledge of strain release in historical events limits the ability to anticipate such behavior. But this does not eliminate the value of concentrating observational effort on regions that likely will experience future very large events, given the success that this strategy has achieved for recent South American earthquakes.

Materials and Methods

Earthquake rupture source dimensions and, for recent events, coseismic slip distributions for ruptures along the South American subduction zone were extracted from the literature. This information is incorporated into Figs. 1 and 2, which document the very large earthquake history dating back to 1500. The rupture lengths for historic events are largely based on documented ground shaking and damage patterns, with information being available for very large events for regional and far-field tsunami inundations. The history of events prior to 1900 is nonuniform along the coast over the past 500 y as it depends on European settlements and archives. In limited regions, sedimentological observations document great events over several millennia. Details of many of the earthquakes extracted from geological, seismological, geodetic, and tsunami observations are discussed and cited in the supplement, with a focus on six recent large events that have been particularly well studied. These observations of the history of large earthquakes along the subduction zone are considered in the context of seismic gap and seismic asperity conceptual models to understand the variation in earthquake ruptures along localized subduction zone segments and to highlight regions with large strain accumulation where future great earthquakes are likely to occur and where geophysical instrumentation can be deployed to capture the later stages of the earthquake cycle culminating in the large events to come.

Data, Materials, and Software Availability. All study data are included in the article and/or SI Appendix. No new data were generated in this study.

ACKNOWLEDGMENTS. We thank Emily Brodsky for discussions of Chilean large earthquake hazard. Sergio Barrientos, Susan Beck, and Lynn Sykes provided helpful reviews. Thorne Lay's research on earthquake processes is supported by the National Science Foundation grant EAR1802364.

Author affiliations: ^aDepartment of Earth and Planetary Sciences, University of California Santa Cruz, Santa Cruz, CA 95064

- H. F. Reid, The mechanics of the earthquake, the California earthquake of April 18, 1906. Report of the State Investigation Commission, Vol. 2 (Carnegie Institution of Washington, Washington D. C., 1910)
- D. Melnick et al., The super-interseismic phase of the megathrust earthquake cycle in Chile. Geophys. Res. Lett. 44, 784-791 (2017), 10.1002/2016GL071845.
- L. R. Sykes, Aftershock zones of great earthquakes, seismicity gaps, and earthquake prediction for Alaska and the Aleutians. J. Geophys. Res. 76, 8021-8041 (1971).
- J. A. Kelleher, L. R. Sykes, J. Oliver, Possible criteria for predicting earthquake locations and their applications to major plate boundaries of the Pacific and the Caribbean. J. Geophys. Res. 78, 2547-2585 (1973).
- B. Schurr et al., The 2007 M7.7 Tocopilla northern Chile earthquake sequence: Implications for along-strike and downdip rupture segmentation and megathrust frictional behavior. J. Geophys. Res. **117**, B05305 (2012), 10.1029/2011JB009030.
- J. C. Villegas-Lanza et al., Nocquet, Active tectonics of Peru: Heterogeneous interseismic coupling along the Nazca megathrust, rigid motion of the Peruvian Sliver, and Subandean shortening accommodation. J. Geophys. Res.: Solid Earth 121, 7371-7394 (2016), 10.1002/2016JB013080.
- S. Ruiz, R. Madariaga, Historical and recent large megathrust earthquakes in Chile. Tectonophysics 733, 37-56 (2018), 10.1016/j.tecto.2018.01.015.
- C. Lomnitz, C., Major earthquakes of Chile: A historical survey, 1535-1960. Seism. Res. Lett. 75, 368-378 (2004), 10.1785/gssrl.75.3.368.
- M. Métois, C. Vigny, A. Socquet, Interseismic coupling, megathrust earthquakes and seismic swarms along the Chilean subduction zone (38°-18°S). Pure Appl. Geophys. 1783, 1431-1449
- T. Lay, H. Kanamori, Earthquake doublets in the Solomon Islands. *Phys. Earth Planet. Int.* **21**, 283-304 (1980).
- 11. T. Lay, H. Kanamori, "An asperity model of large earthquake sequences" in Earthquake Prediction An International Review, D. W. Simpson, P. G. Richards, Eds. (Maurice Ewing Series, 4, AGU, Washington D.C., 1981), (4), pp. 579-592.
- T. Lay, H. Kanamori, L. Ruff, The asperity model and the nature of large subduction zone earthquakes. Earthquake Pred. Res. 1, 3-71 (1982).
- K. Aki, Characteristics of barriers on an earthquake fault. J. Geophys. Res. 84, 6140-6148 (1979).
- C. H. Scholz, Earthquakes and friction laws. Nature 391, 37-42 (1998), 10.1038/34097
- M. W. Herman, K. P. Furlong, R. Govers, The accumulation of slip deficit in subduction zones in the absence of mechanical coupling: Implications for the behavior of megathrust earthquakes. J. Geophys. Res. 123, 8260-8278 (2018), 10.1029/2018JB016336.
- J. A. Kelleher, Rupture zones of large South American earthquakes and some predictions. J. Geophys. Res. 77, 2087-2103 (1972).
- W. R. McCann, S. P. Nishenko, L. R. Sykes, J. Krause, Seismic gaps and plate tectonics: Seismic potential for major boundaries. *Pure Appl. Geophys.* 117, 1082–1147 (1979), 10.1007/ BF00876211.
- S. P. Nishenko, Seismic potential for large and great interplate earthquakes along the Chilean and southern Peruvian margins of South America: A quantitative reappraisal. J. Geophys. Res. 90, 3589–3615 (1985), 10.1029/JB090iB05p03589.
- S. P. Nishenko, Circum-Pacific seismic potential: 1989–1999. Pure Appl. Geophys. 135, 169–259 (1991).
- Y. Y. Kagan, D. D. Jackson, Seismic gap hypothesis: Ten years after. J. Geophys. Res. 96, 21419-21431 (1991).
- S. P. Nishenko, L. R. Sykes, Comment on "Seismic gap hypothesis: Ten years after" by Y. Y. Kagan and D. D. Jackson. J. Geophys. Res. 98, 9909-9916 (1993).
- Y. Y. Kagan, D. D. Jackson, New seismic gap hypothesis: Five years after. J. Geophys. Res. 100, 3943-3960 (1995).
- Y. Y. Kagan, D. D. Jackson, R. J. Geller, Characteristic earthquake model, 1884-2011, R.I.P., opinion. Seism. Res. Lett. 83, 951-953 (2012).
- T. Lay, The surge of great earthquakes from 2004 to 2014. Earth Planet. Sci. Lett. 409, 133-146 (2015).
- 25. H. Kanamori, K. C. McNally, Variable rupture mode of the subduction zone along the Ecuador-Colombia coast. Bull. Seism. Soc. Am. 72, 1241-1253 (1982).
- M. Chlieh et al., Distribution of discrete seismic asperities and aseismic slip along the Ecuadorian megathrust. Earth Planet. Sci. Lett. 400, 292–301 (2014), 10.1016/j.epsl.2014.05.027. L. Ye et al., The 16 April 2016, M_W 7.8 (M_S 7.5) ecuador earthquake: A quasi-repeater of the 1942
- M_S 7.5 earthquake and partial re-rupture of the 1906 M_S 8.6 Colombia-Ecuador earthquake. Earth Planet. Sci. Lett. 454, 248–258 (2016), 10.1016/j.epsl.2016.09.006.
- 28. P. A. Mothes et al., Monitoring the earthquake cycle in the northern Andes from the Ecuadorian cGPS network. Seismol. Res. Lett. 89, 534-541 (2018), 10.1785/0220170243.
- M. Chlieh et al., Interseismic coupling and seismic potential along the Central Andes subduction zone. J. Geophys. Res. 116, B12405 (2011), 10.1029/2010JB008166.
- V. Yanez-Cuadra et al., Interplate coupling and seismic potential in the Atacama Seismic Gap (Chile): Dismissing a rigid Andean sliver. Geophy. Res. Lett. 49, e2022GL098257 (2022), 10.1029/2022GL098257.
- 31. L. Dorbath, A. Cisternas, C. Dorbath, Assessment of the size of large and great historical earthquakes in Peru. Bull. Seism. Soc. Am. 80, 551-576 (1990), 10.1785/BSSA0800030551.

- 32. T. Lay, C. J. Ammon, A. R. Hutko, H. Kanamori, Effects of kinematic constraints on teleseismic finitesource rupture inversions: Great Peruvian earthquakes of 23 June 2001 and 15 August 2007. Bull. Seism. Soc. Am. 100, 969-994 (2010), 10.1785/0120090274.
- 33. H. Perfettini et al., Seismic and aseismic slip on the Central Peru megathrust. Nature 465, 78-81 (2010), 10.1038/nature09062.
- M. K. Giovanni, S. L. Beck, L. Wagner, The June 23, 2001 Peru earthquake and the Southern Peru subduction zone. Geophys. Res. Lett. 29, 14-1-14-4 (2002), 10.1029/2002GL015774.
- C. Jiménez, C. Carbonel, J. C. Villegas-Lanza, Seismic source of the earthquake of Camana Peru 2001 (M_W 8.2) from joint inversion of geodetic and tsunami data. *Pure Appl. Geophys.* **178**, 4763–4775 (2021), 10.1007/s00024-020-02616-8.
- S. Ruiz et al., Intense foreshocks and a slow slip event preceded the 2014 Iquique M_W 8.1 earthquake. Science **345**, 1165–1169 (2014), 10.1126/science.1256074.
- B. Schurr et al., Gradual unlocking of plate boundary controlled initiation of the 2014 Iquique earthquake. Nature 512, 299-302 (2014), 10.1038/nature13681.
- Y. Bai, K. F. Cheung, Y. Yamazaki, T. Lay, L. Ye, Tsunami surges around the Hawaiian Islands from the 1 April 2014 North Chile MW 8.1 earthquake. Geophys. Res. Lett. 41, 8512-8521 (2014), 10.1002/2014GL061686.
- G. P. Hayes et al., Continuing megathrust earthquake potential in Chile after the 2014 Iquique earthquake. Nature 512, 295-298 (2014), 10.1038/nature13677.
- F. Hoffmann et al., Characterizing afterslip and ground displacement rate increase following the 2014 Iquique-Pisagua M_W 8.1 earthquake, Northern Chile. J. Geophys. Res.: Solid Earth 123, 4171-4192 (2018), 10.1002/2017JB014970.
- 41. E. Kausel, Los terremotos de Agosto de 1868 y Mayo de 1877 que afectaron el sur del Perú y norte de Chile. Boletín de la Academia Chilena de Ciencias 3, 8-13 (1986).
- D. Comte, M. Pardo, Reappraisal of great historical earthquakes in the Northern Chile and Southern Peru seismic gaps. Nat. Haz. 4, 23-44 (1991).
- C. Vigny, E. Klein, The 1877 megathrust earthquake of North Chile two times smaller than thought? A review of ancient articles. J. S. Amer. Earth Sci. 117, 103878 (2022), 10.1016/j. jsames.2022.103878.
- S. Beck, S. Barrientos, E. Kausel, M. Reyes, Source characteristics of historic earthquakes along the central Chile subduction zone. J. South Am. Earth Sci. 11, 115-129 (1998).
- L. Ye, T. Lay, H. Kanamori, K. D. Koper, Rapidly estimated seismic source parameters for the 16 September 2015 Illapel Chile M_W 8.3 earthquake. Pure Appl. Geophys. 173, 321–332 (2016), 10.1007/s00024-015-1202-y.
- L. Li, T. Lay, K. F. Cheung, L. Ye, Joint modeling of teleseismic and tsunami wave observations to constrain the 16 September 2015 Illapel, Chile, M_W 8.3 earthquake rupture process. Geophys. Res. Lett. 43, 4303-4312 (2016), 10.1002/2016GL068674.
- 47. M. W. Herman et al., Integrated geophysical characteristics of the 2015 Illapel, Chile, earthquake. J. Geophys. Res.: Solid Earth **122**, 4691-4711 (2017), 10.1002/2016JB013617.
- 48. G. Easton et al., Complex rupture of the 2015 M_W 8.3 Illapel earthquake and prehistoric events in the Central Chile tsunami gap. Seis. Res. Lett. 93, 1479-1496 (2022), 10.1785/0220210283.
- M. Métois, C. Vigny, A. Socquet, Interseismic coupling, megathrust earthquakes and seismic swarms along the Chilean subduction zone (38°-18°S). Pure Appl. Geophys. 1783, 1431–1449 (2016)
- F. Tilmann et al., The 2015 Illapel earthquake, central Chile: A type case for a characteristic earthquake? Geophys. Res. Lett. 43, 574-583 (2016), 10.1002/2015GL066963.
- H. Huang, W. Xu, L. Meng, R. Burgmann, J. C. Baez, Early aftershocks and afterslip surrounding the 2015 M_W 8.4 Illapel rupture. Earth Planet Sci. Lett. 457, 282-291 (2017), 10.1016/j. epsl.2016.09.055.
- 52. H. Yue et al., Localized fault slip to the trench in the 2010 Maule, Chile M_W 8.8 earthquake from joint inversion of high-rate GPS, teleseismic body waves, InSAR campaign GPS, and tsunami observations. J. Geophys. Res. 119, 7786-7804 (2014), 10.1002/2014JB011340.
- F. Romano et al., Benchmarking the optimal time alignment of tsunami waveforms in nonlinear joint inversions for the Mw, 8.8 2010 Maule (Chile) earthquake. Front. Earth Sci. 8, 585429 (2020), 10.3389/feart.2020.585429.
- M. Métois, A. Socquet, C. Vigny, Interseismic coupling, segmentation and mechanical behavior of the central Chile subduction zone. J. Geophys. Res. 117, B03406 (2012), 10.1029/2011JB008736.
- S. Lorito et al., Limited overlap between the seismic gap and coseismic slip of the great 2010 Chile earthquake. Nat. Geosci. 4, 173-177 (2011), 10.1038/ngeo1073.
- E. Klein, L. Fleitout, C. Vigny, J. D. Garaud, Afterslip and viscoelastic relaxation model inferred rom the large-scale post-seismic deformation following the 2010 M_W 8.8 Maule earthquake (Chile). Geophys. J. Int. 205, 1455-1472 (2016), 10.1093/gji/ggw086.
- 57. J. F. Pacheco, L. R. Sykes, C. H. Scholz, Nature of seismic coupling along simple plate boundaries of the subduction type. J. Geophys. Res. 98, 14133-14159 (1993).
- N. Uchida, T. Matsuzawa, Coupling coefficient, hierarchical structure, and earthquake cycle for the source area of the 2011 off the Pacific coast of Tohoku earthquake inferred from small repeating earthquake data. Earth Planets. Space 63, 675-679 (2011).
- T. Lay et al., Depth-varying rupture properties of subduction megathrust faults. J. Geophys. Res. 117, B04311 (2012), 10.1029/2011JB009133.

- J. A. Kelleher, W. R. McCann, Buoyant zones, great earthquakes, and unstable boundaries of subduction. *J. Geophys. Res.* 81, 4885–4908 (1976).
 N. Wetzler, T. Lay, E. E. Brodsky, H. Kanamori, Rupture-depth-varying seismicity patterns for major and great (M_W ≥ 7.0) megathrust earthquakes. *Geophys. Res. Lett.* 44, 9663–9671 (2017), 10.1002/2017GL074573.
- 62. J. P. Loveless, M. E. Pritchard, N. Kukowski, Testing mechanisms of subduction zone segmentation
- D. F. Loveless, M. E. Fritchado, N. Nakowski, lesting internalishs of subduction zone segmentation and seismogenesis with slip distributions from recent Andean earthquakes. *Tectonophysics* 495, 15–33 (2010), 10.1016/j.tecto.2009.05.008.
 M. W. Herman, R. Govers, Locating fully locked asperities along the South America subduction megathrust: A new physical inter-seismic inversion approach in a Bayesian framework. *Geochem. Geophys. Geosys.* 21, e2020GC009063 (2020).
- 64. D. Comte et al., Seismicity an stress distribution in the Copiapo, northern Chile Subduction zone using combined on- and off-shore seismic observations. *Phys. Earth Planet. Int.* **132**, 197–217 (2002), 10.1016/S0031-9201(02)00052-3.
- H. Kanamori et al., New constraints on the 1922 Atacama, Chile, earthquake from historical seismograms. Geophys. J. Int. 219, 645-661 (2019), 10.1093/gji/ggz302.
 M. Carvajal et al., Reexamination of the magnitudes for the 1906 and 1922 Chilean earthquake
- Mr. Carvajal et al., Reexamination of the inaginitudes for the 1900 and 1922 Clinical earthquake using Japanese tsunami amplitudes: Implications for source depth constraints. J. Geophys. Res.: Solid Earth 122, 4-17 (2016), 10.1002/2016JB013269.
 L. R. Sykes, Decadal seismicity prior to great earthquakes at subduction zones: Roles of major asperities and low-coupling zones. Int. J. Geosci. 12, 845–926 (2021), 10.4236/iii. 2021.12004.
- ijg.2021.129046.

Updated concepts of seismic gaps and asperities to assess great earthquake hazard along South America

Thorne Lay^{a,*} and Stuart P. Nishenko

Supporting Information

6 Ecuador-Colombia

- 7 The Ecuador-Colombia plate boundary from 4°N to 3°S (Figure 1) involves oblique underthrusting of the
- 8 Nazca plate at ~4.6 cm/yr below the North Andean Sliver, a fragment of the South American plate (1-3).
- 9 The broad Carnegie Ridge on the incoming oceanic plate intersects the subduction zone from 0.5°N to
- 10 2.0°S (4). Modeling of interseismic geodetic strain around the megathrust requires accounting for the
- movement of the sliver relative to stable South America along with any distributed deformation in the
- northern Andes. Doing so indicates heterogeneous locking of the plate interface from 3°N to 3°S, with
- relatively uniform >40% locking north of 0.5°S and an isolated patch below La Plata Island from 1°S to
- 1.5°S where a slow-slip event occurred in 2010 and no large $(M_W > 7)$ earthquake has been recorded (2; 5-
- **15 7**).

1

2

3

4

- The history of very large megathrust earthquakes along this region is relatively short (Figure 2a). The
- 17 1906 M_w 8.6 Columbia/Ecuador earthquake is the largest known event. It had an estimated rupture length
- of \sim 500 km, based on macroseismic data (8), and produced significant local and Pacific wide tsunami (M_T
- 19 8.7, 9). Historic information on earlier events provide only indirect evidence for recurrence times in that
- 20 no event comparable to 1906 is recorded in the historic catalog from 1575 to 1915 (331 years) (10).
- 21 Earthquake triggered turbidites collected on the continental slope offshore of Esmeraldas River indicate
- 22 that one or two earthquakes comparable in size to the 1906 event occurred ~600 years ago (11).
- A series of great earthquakes re-ruptured the near coastal portion of the 1906 Colombia/Ecuador zone
- within 36 (1942, M_S 7.5), 52 (1958, M_S 7.3) and 73 (1979, M_S 7.7) years of 1906 (12). An M_W 7.1 event in
- 25 1998 ruptured the southernmost portion of the 1906 zone southwest of the 1942 rupture (2). The
- aftershock zones of these ruptures abut without overlap within the larger 1906 rupture zone (13). Analysis
- of seismic waveforms (14) and GPS data (2) has identified discreet asperities associated with the 1958
- and 1979 ruptures. Kanamori and McNally (12) note that the cumulative seismic moment of the 1942,
- 29 1958 and 1979 earthquakes based on aftershock zone area is considerably less (~1/5) than the seismic
- moment of 1906. This discrepancy reduces to $\sim 1/3$ based on direct waveform comparisons (14).
- 31 The re-rupture of the 1942 Pedernales, Ecuador segment in 2016 (M_W 7.8, M_S 7.5) presents an opportunity
- 32 to examine persistent heterogeneous frictional properties of the Colombia-Ecuador megathrust, and may
- indicate the onset of a new earthquake cycle along the Colombia-Ecuador region.
- 34 *2016 Ecuador*
- 35 The 16 April 2016 M_W 7.8 Pedernales, Ecuador earthquake (Figures 1, 2a, 3a) ruptured the down-dip
- portion of the Colombia/Ecuador seismogenic zone along prior ruptures in 1906 (M_W 8.6) and 1942 (M_W
- 37 (7.8). The source region had previously been accumulating moderate slip deficit based on geodetic
- 38 measurements (2), with larger slip deficit accumulating in the adjacent regions of non-overlapping
- aftershock zones of the 1958 (M_W 7.6) and 1979 (M_W 8.1) ruptures, extending along the 1906 zone. Chlieh

et al. (2) estimated characteristic earthquake recurrence times for asperities associated with 1942, 1958 and 1979 events of ~140±30, 90±20 and 153±80 years, respectively, significantly exceeding their actual intervals since 1906 (36, 52, and 73 years). After 74 years, the 1942 region re-ruptured in the 2016 event.

Available high-rate GPS, broadband teleseismic, InSAR, and tsunami data resolve the rupture of two large-slip patches in 2016 with peak slip of \sim 2-6 m and an average slip \sim 2 m (6, 15-18). Comparison of seismic waveforms and magnitudes demonstrate that the 2016 and 1942 events have similar surface wave magnitudes (M_S 7.5), overlapping rupture areas, and an overlapping large-slip patch, but not identical teleseismic waveforms – indicating that 2016 was a quasi-repeat of 1942 (15, 19). While the average slip in 2016 is consistent with the plausible slip deficit accumulation of 3.5 m since 1942, given the \sim 4.7 cm/yr convergence rate (15), localized peak slip estimates of 5-6 m exceed the expected slip deficit (6), indicating that significant residual slip deficit persisted after the 1942 event in the localized region of peak slip in 2016. Nocquet et al. (6) also infer excessive moment release in the 1958 and 1979 events relative to slip deficits accumulated since 1906. Noting the lack of historic large earthquakes in the region (Figure 2a), they propose that the Ecuador-Colombia region has been experiencing a supercycle of large events over the past century. Yoshimoto et al. (18) invert for the tsunami source of 1906, finding large-slip on the shallow megathrust, up-dip of the large-slip zones in 2016, 1942, 1958 and 1979, complicating assessment of strain budget for localized regions of the megathrust.

PERU

 The Peru seismic zone, extending from 3°S to ~19°S, has the most pronounced variability in very large megathrust faulting history of the entire South American seismogenic zone (Figures 1, 2b). The Northern Peru segment from 3°S to 10°S is bounded by the Grihalva Ridge to the north and the Mendaña Fracture zone to the south. Geodetic measurements in the region (1, 20-21) indicate that the plate boundary is not accumulating significant slip deficit along the 800-km-long segment other than in localized shallow (<20 km deep), poorly resolved patches near 3°S-4°S and 7°S-8°S. The area near Chimbote (~9°S) has experienced infrequent large earthquakes (Figure 2b), the largest being $M_W \sim 7.7$ -8 in 1619 (8; 21-23). That event destroyed the town of Trujillo and macroseismic reports indicate that damage extended over 100-150 km. The most recent large events along Northern Peru are the 1960 M_W 7.6 and 1996 M_W 7.5 earthquakes located on the shallow megathrust (Figure 1, 2b), which have both been characterized as tsunami earthquakes due to having weak radiation of short-period seismic energy, low rupture velocity and long rupture durations (24-27). Future occurrence of very large earthquakes in this region is very difficult to anticipate based on the coupling and historical records.

The seismic record for central and southern coastal Peru (Figure 2b) is considered complete for earthquakes of M > 7.6 for more than 450 yr (21-23; 28). The Central Peru segment from 10°S to 14.5°S is bounded by the Mendaña Fracture Zone to the north and the Nazca Ridge to the south. The subducted Nazca plate in central Peru is characterized by flat, low angle subduction and a lack of active volcanism. Dorbath et al. (23) describe the seismic activity in Central Peru as being complex due to the irregularity of rupture lengths, locations of epicentral zones, and timing. Two earthquakes stand out in the historic record, not only for their size but also for the length of time of seismic quiescence following their occurrence. The 1687 M_W 8.4 Ica earthquake ruptured the southern half of the central Peru segment with an estimated rupture length of 350 km and produced a damaging local tsunami with a height of 5 to 10 m $(M_T 8.5-8.4, 9)$. The 1746 $M_W 8.6$ Lima, Peru earthquake ruptured the northern 350 km of the central Peru segment 59 years later with long overlap of the 1687 zone and produced a local tsunami of 15 to 24 m height $(M_T 9 - 9.2, 9)$. The 1746 event ranks as the largest Peruvian earthquake during the last 450 years (23) and coupled with the earlier 1687 earthquake (the slip distributions are not known in detail) may represent a so-called "Breakthrough Event" (29) that ruptured the entire Central Peru segment (30). Following these two events, a period of seismic quiescence for great earthquakes along much of Central Peru lasted nearly 200 years (23).

A renewed period of earthquake activity spanning Central Peru started in 1940. A series of great earthquakes progressively re-ruptured portions of the 1687 and 1746 zones in 1940 $(M_W 8.2)$, 1966 $(M_W$ 88 89 8.1), 1974 (M_W 8.1) and 2007 (M_W 8.0) (8; 22-23; 30-31). These recent events occurred at intermediate 90 depths along the megathrust (15 to 35 km), and exhibit non-overlapping rupture zones (Figures 1, 2b) consistent with the seismic gap and asperity concepts. Waveform analysis of these events (18, 31-35) 91 92 identified one to three concentrated large-slip zones, or asperities, for each event. The events produced minor local tsunamis ranging from 1.6 to 3 m in height that were significantly less than those reported for 93 1687 and 1746. This is similar to the Ecuador-Colombia region. Chlieh et al. (36) estimate that the recent 94 95 set of events account for less than half of the estimated seismic moment release in 1746, leaving a deficit that could produce an M_W 8.5-8.7 event. The 2007 rupture struck the southeastern end of this region, 96 97 which had not had a very large earthquake since 1746.

- 98 *2007 Pisco, Peru*
- The 15 August 2007 (M_W 8.0) Pisco, Peru earthquake produced substantial shaking damage and a large tsunami on the southern Paracas peninsula (Figures 1, 2b, 3b), northwest of the intersection of the Nazca Ridge with the Peru Trench. The seismic, geodetic and tsunami data for this event reveal that the rupture involved two or more large-slip patches straddling the peninsula with about a 60 s lag time between the primary subevents (e.g., 20; 34-43). Maximum slip was up to about 8 m and geodetic slip deficit had been observed prior to the rupture (36).
- The discrete ruptures during this event, with two main separated asperities experiencing triggering 105 interaction and adjacent up-dip and along-strike afterslip with seismic moment equal to 14% of the co-106 107 seismic moment (20) are consistent with the asperity model, but this type of multi-asperity delayed 108 rupture presents great challenges to early warning procedures that attempt to characterize imminent 109 seismic and tsunami hazards from the early energy release or ground deformation (34). Longer term, interseismic coupling models indicate as much as 50-70% aseismic slip in this region and are consistent 110 with return times of 250 years or greater (i.e., 2007 - 1687 = 261 yrs), in this region just north of where 111 112 the Nazca ridge intersects the subduction zone (20). Given the lack of seismic recordings of prior events striking the recent rupture zones, we cannot assess persistence of asperities in Central Peru. 113
- The Southern Peru segment extends from 14.5° S, where the Nazca Ridge intersects the trench, to ~19°S, near the Chilean border and Arica. Great earthquakes have occurred relatively frequently in Southern Peru (22-23; 44) during the last 500+ years (Figure 2b). Great ruptures spanning this segment struck in 1604 and 1868, with pairs of very large events (1687/1715 and 1784/1833) also covering most of the length. The region in the north near the city of Nazca had several large ruptures in 1913, 1942 (M_W 8.1) and 1996, with the latter two being partially overlapping complex ruptures along the southern flank of the Nazca Ridge intersection (19; 45).
- 121 2001 Southern Peru

- The 23 June 2001 M_W 8.4 Arequipa (or Camaná), Peru earthquake and its magnitude 7.6 aftershock on 7 July 2001 to the southeast, re-ruptured the northern two-thirds of the 1868 seismic gap (Figures 1, 2b, 3b). Based on analysis of seismic, geodetic and tsunami data, the earthquake broke two spatially offset asperities, the first in the northwest of the rupture zone and the second, centrally located asperity being much larger and releasing most of the total seismic moment (34; 36-37; 46-49). Rupture appears to have extended across the megathrust to near the trench (34; 36), unlike the 2007 Pisco and 2016 Ecuador events.
- Earthquake intensity and tsunami runup reports indicate that great events in 1604 and 1868 (10-15 m and 14 m peak tsunami runup, respectively) were larger than the overlapping 1582, 1784, and 2001

earthquakes (1-2 m, 2-4 m, and 8.8 m peak tsunami runup, respectively) (Figure 2b) (23; 46). Lacking 132 seismic recordings it is not possible to compare details of the ruptures or to assess persistence of 133 134 asperities, but the repeated occurrence of great earthquakes with overlapping ruptures is consistent with 135 the basic seismic gap concept, with frictional heterogeneity resulting in smaller slip patches adjacent to a large central asperity. The 1604 and 1868 MMI VIII isoseismal zones both extend farther southeast 136 137 toward Arica, Chile than the 2001 ruptures, indicating that the southeasternmost portion of the Peru plate boundary has remained unbroken for 154 years (46; 50-51). Geodetic slip deficit accumulation in the area 138 is high (~63 mm/yr) indicating that as much as ~10 m of slip may have accumulated in the region since 139 1868, with potential seismic moment equivalent to an M_W 8.4 event. It is unclear why the 2001 event 140 failed to rupture into this region, but there is evidence for prior smaller events that ruptured just this 141 region in 1833 and 1715 (Figure 2b). 142

143 CHILE

144 Northern Chile

- The Northern Chile region extending from 19°S to 26°S has a limited very large earthquake history, 145 dominated by the great 1877 (M_W 8.5-8.8) and 1995 Antofagasta (M_W 8.0) earthquakes (Figures 1, 2c) 146 147 (52). Large events for which there is some information struck northernmost Chile in 1615, 1768 and 1786, in the vicinity of the recent 2014 Iquique event (44). There is marine evidence for slumping near 148 23°S occurring between 1754 and 1789 (53), indicating that the 1768 and/or 1786 ruptures may have 149 extended along the entire 1877 zone. Marine evidence near 23°S and boulder fields on the Atacama coast 150 also indicate a predecessor event overlapping the 1877 event around 1429 ± 20 (53, 54), coincident with 151 152 Japanese tsunami records of a distant event on 7 September 1420 (55). Geologic and archeological provide evidence for a giant $(M \sim 9.5)$ earthquake in this region at ~ 3800 years ago (56) that may have 153 also affected the Northern Chile and Atacama Desert region from 21° to 27° S. 154
- 155 *2014 Iquique, Chile*

163

164165

166

167

168169

170

171

172

173174

175

176

The 1 April 2014 Mw 8.1 Iquique, Chile earthquake and its large M_W 7.7 aftershock on 3 April 2014 to the south ruptured a rather compact area of the northern Chile central megathrust from 19.3°S to 20.7°S (Figures 1, 2c, 3c). The large-slip zone (~2-7 m) for the 2014 mainshock is unusually concentrated for a great earthquake, extending only about 70 km along strike and 50 km along-dip, with finite-slip models being well resolved by seismic, geodetic, and tsunami observations (57-64). The rupture was preceded by months of slowly migrating foreshock activity located up-dip of the eventual mainshock, indicating along-dip variation in frictional properties of the megathrust (59; 65-71)

The concentrated mainshock slip, with adjacent down-dip slow deformation and afterslip (71; 72) is consistent with the asperity model, and several prior historical earthquakes have occurred in this region of northernmost Chile over the past few centuries (Figure 2c), so persistence of localized velocity weakening properties is viable. The event struck in an area of large slip deficit inferred from geodesy that extends along northern Chile from 18°S to 25°S, with a low coupling zone near 21°S (36; 72-74), although the coupling estimates depend strongly on assumptions of upper plate (central Andes) distributed deformation. Many estimates of the 1877 rupture extent span this region (e.g., 44; 75), so early interpretations viewed the 2014 event as a partial rupture of the 1877 zone akin to the events along Ecuador-Colombia. However, based on detailed reinterpretation of intensity observations for 1877, the 2014 Iquique event, rupturing the megathrust region south of Arica and north of Iquique lies between large-slip regions of the great 1868 and 1877 earthquakes (76) (Figure 3c). The 1877 slip zone may or may or may not have overlapped the 2014 event, and while it extends along the 2007 Tocopilla event at its southern end (Figure 2c), the latter event was concentrated down-dip in Domain C and did not rupture the shallow megathrust (36; 77-80).

177 1995 Antofagasta

The 30 July 1995 M_W 8.0 Antofagasta earthquake ruptured south of the 1877 earthquake gap from 23.3°S 178 to 25°S (Figures 1, 2c, 3d). Analysis of seismic, geodetic, and tsunami data indicate that the rupture 179 began near the Mejillones peninsula and expanded southward with predominantly unilateral slip (81-88), 180 to the vicinity of the 1966 (M_S 7.8) Tal-Tal earthquake at its southern end. Long-period directivity 181 182 indicates a rupture velocity of 3.0-3.2 km/s and rupture duration of 60-68 s (85). The finite-fault studies 183 resolve slip beneath the coastal area in the central megathrust (Domain B of Figure 4), with some alongstrike variability that may be due to prior stress relaxation in 1987 (M_W 7.5) and 1988 (M_W 7.2) ruptures 184 and a 1998 (M_W 7.0) aftershock in the deeper portion of the megathrust (Domain C of Figure 4) (87; 89). 185 The rupture south of 24.3°S appears to have modest slip that extends to near the trench (Domain A of 186 187 Figure 4) based on strong excitation of pwP arrivals (27, 90), and there is some indication of this in finite-188 fault modeling, although such models lack resolution of slip near the trench (88).

189 North-Central Chile - Atacama

190 Seismic waveform modeling (91) indicates rupture of 3 sub-events during the 1922 Atacama earthquake. consistent with eyewitness accounts of feeling three distinct shocks within the first few minutes. The prior 191 192 great rupture in 1819 involved a sequence of three events on April 3, 4 and 11, as well (92). As seen in 193 Figure 3d, a line of seamounts intersects the Chile trench near 27°S, in the northern portion of the 1922 194 Atacama earthquake rupture zone which has had repeated smaller events in 1851, 1859, 1918, 1946 and 1983 (Figure 2c). The seamounts are spaced ~ 100 to 150 km apart and are ~25 km in diameter. Each 195 seamount or asperity could accumulate a slip deficit of 6 to 7 m per century, equivalent to an M 7+ 196 197 earthquake. While the seismic moments of subevents in 1922 are not well constrained (91, 93), the rough 198 seafloor bathymetry may account for some of the rupture complexity. Evidence for prior great ruptures 199 from paleotsunami run-up along the Atacama include the 1429 ± 20 event (53; 54) discussed above, along with 1267 ± 85 ? and 964 ± 32 ? segment-spanning events (94). 200

201 Central Chile

The Illapel region (30°S-32°S) (Figures 1, 3e) is a highly coupled segment of central Chile bounded by 202 the Challenger Fracture Zone (CFZ) to the north and the Juan Fernandez Ridge (JFR) to the south (95-203 97). The CFZ intersects the Chile Trench near the southern end of the 1922 Atacama earthquake and at 204 205 the estimated northern end of the great 1730 Valparaíso earthquake, suggesting persistent segmentation. The Illapel segment exhibits complexity of very large earthquake rupture as it ruptured in the northern 206 207 \sim 1/3 of the great 1730 $M_W \sim$ 9 Valparaíso earthquake as well as in a series of smaller overlapping events 208 in 1880 (M_W 8.3), 1943 (M_W 7.9), and 2015 (M_W 8.3). The latter set of ruptures may possibly involve a 209 persistent asperity on the central megathrust, but with variable amounts of shallow coseismic slip near the 210 trench. There is no clear data on great events prior to 1730, extending south to Constitución.

211 *2015 Illapel, Chile*

212 The 16 September 2015 M_W 8.3 Illapel, Chile earthquake ruptured ~170 km along the plate boundary megathrust in Central Chile from 30°S to 31.6° S (Figure 1). This event struck in the same region as 213 events in 1943, 1880, and 1730 (Figures 2c, 3e) (8; 91; 98-99). The 2015 Illapel earthquake is of 214 particular note because rapid seismic magnitude estimation of the event prompted a tsunami warning and 215 evacuation notifications within 8 to 11 min of the origin time, resulting in large-scale evacuation along 216 the Chile coast (100). Seismic, geodetic, and tsunami waveform analyses of the 2015 Illapel earthquake 217 indicate concentrations of \sim 3 m co-seismic slip below the coast and an large patch with up to \sim 10 m slip 218 219 at shallow depths (94; 100-113). Studies with the best off-shore resolution (including careful modeling of 220 tsunami arrivals) are consistent with the large-slip patch having extended up-dip to near the trench.

Geodetic measurements prior to the event indicate that there was strong megathrust coupling in the region of large-slip, particularly south of 31°S, although resolution of coupling out to the trench is very low (106; 114-115), and afterslip expanded both northward and southward from the large-slip zone (110; 116-118).

Similar to the 2016 Ecuador earthquake, comparisons can be made with details of the prior very large rupture in 1943. The 1943 M_W 7.9 event has a single pulse of large moment rate at depths < 35 km but has a much smaller seismic moment estimate and simpler waveforms that indicate that it did not rupture the shallow portion of the megathrust (91; 101). Local tsunami heights for the 2015 event are significantly higher than those in 1943, and ranged from 3 to 6 m along the coast from 29°S to 32°S, with localized peak values of 13 m at La Cebada (30.98°S, 71.65°W) and 10.8m at Totoral (30.37°S, 71.67°W) and a tide gauge peak recording of 4.5 m at Coquimbo to the north (119; 120). Far-field tsunami amplitudes reported in Japan for the 1943 event (10-30 cm, 91) are less than those reported in 2015 (11-80 cm). The macroseismic effects of the 1943 earthquake are broadly similar to the 2015 event, but extend further south. (8: 91). Aftershocks for the 1943 event, located by Kelleher (8) using S-P times from La Paz, indicate along-strike rupture zone dimension comparable to 2015 (106). Peak slip in 2015 (8-12 m) is greater than the slip accumulated during the interval 1943-2015 (5.3 m for 74 mm/yr convergence) although average slip is comparable. Overall, the 2015 event is not a simple repeat of the 1943 event and likely had much more slip at shallow depth (100). The 1880 rupture was similar in extent, but the 1730 rupture extended much further to the south, akin to the Ecuador-Colombia behavior. While there may be persistent asperities in the central and shallow megathrust, they may fail independently in some events and may participate in along-strike cascades in other events (106).

2010 Maule, Chile

The 27 February 2010 Maule (M_W 8.8) earthquake ruptured the plate boundary offshore of central Chile between 34°S and 38.5°S (Figure 1, 3f). The coseismic slip of this event has been determined by analysis of seismic, geodetic, and tsunami observations (121-134). Patchy coseismic slip is distributed over a region 460 km long and 100 km wide between the depths of 15 and 40 km. Two large-slip asperity regions are resolved along the megathrust, one extending from 34°S to 36°S (with up to 20 m slip) and the other from 37°S to 38°S (with up to 10 m slip). Finite fault inversions relying on only on-land static geodetic data tend to place slip on the central megathrust toward the coastline (124; 125; 131), but (132) and (134) find that the large-slip patches include slip of 5-8 m all the way to the trench based on joint inversions with accurately modeled tsunami observations. This is consistent with direct images of coseismic seafloor displacement at the trench from repeated seismic reflection surveys (135). Concentrations of outer trench-slope normal faulting occurred offshore from these shallow slip patches (132). Aftershocks concentrate along the down-dip megathrusts and around the large-slip zones (136).

Geodetic measurements had resolved accumulating slip deficit prior to the rupture along the entire rupture area, with moderate reduction near 35°S (95; 114; 123; 131; 137), but the patchy slip distribution only loosely conforms to the variable geodetic locking distribution (138). Afterslip extends along the length of the rupture primarily down-dip and between the two large coseismic slip patches (126; 131; 139-140). While the region was recognized as a seismic gap along the historic 1835 rupture zone and geophysical instrumentation was deployed in the region in advance of the earthquake, the co-seismic slip was moderate in the 1835 source area. Substantial slip overlapped the 1928 rupture zone and slip terminated adjacent to the 1985 rupture zone (141). The estimated slip deficit from 1835 to 2010 is ~12 m, somewhat above the average slip in the southern half of the rupture zone. Much less slip deficit could have accumulated after 1928, but that event could have ruptured the deeper megathrust, below the region of 20 m slip in 2010, with large ruptures in 1647, 1730 and 1751 possibly having ruptured the same region (Figure 2c). Conventional seismic gap ideas with strong segmentation do not characterize this

- region well, but the Reid strain renewal concept in conjunction with a distribution of persistent asperities
- along the megathrust reconciles the historical behavior.
- 270 Southern Chile
- Southern Chile (Figures 1, 2d), extending from 38°S near the Arauco Peninsula to 48°S near the 271 intersection with the Chile Rise has hosted several great historic megathrust ruptures in 1575, 1737 and 272 273 1837 (52; 92; 142; 143), as well as the 1960 M_W 9.5 event (144-150). It appears that the 1737 and 1837 274 events had limited overlap (Figure 2d), and together spanned the 1575 and 1960 rupture extent (52). Paleotsunami evidence indicates ruptures preceding 1575 in $1337 \pm 18(?)$ and 1154 ± 27 (94), with 275 biostratigraphy giving compatible dates of 1270-1450 and 1070-1220 (151). A recurrence time of about 276 270 years appears to hold along this segment (142; 152). Dura et al. (152) also consider whether the 277 Arauco Peninsula (37°-38°S) is a persistent barrier. The 2010 Maule event ruptured into, but not across 278 this region, and the 1835, 1751, 1657 and 1570 events in Central Chile also did not cross it, nor did the 279 1960, 1737 and 1575 events to the south, so it appears to have been a persistent impediment to through-280
- going rupture over the last 600 years.

282 Supplemental Refs

- 1. J.-M. Nocquet, J. C. Villegas-Lanza, M. Chlieh, P. A. Mothes, F. Rolandone, P. Jarrin et al., Motion of continental slivers and creeping subduction in the northern Andes. *Nat. Geosci.*, 7,
- 285 287-291 (2014). https://doi.org/10.1038/NGEO2099.
- M. Chlieh, P. A. Mothes, J.-M. Nocquet, P. Jarrin, P. Charvis, D. Cisneros, et al., Distribution of discrete seismic asperities and aseismic slip along the Ecuadorian megathrust. *Earth Planet. Sci. Lett.* 400, 292-301 (2014). https://doi.org/10.1016/j.epsl.2014.05.027.
- 3. A. Alvarado, L. Audin, J. M. Nocquet, E. Jaillard, P. Mothes, P. A. Jarrín, et al. Partitioning of oblique convergence in the Northern Andes subduction zone: Migration history and the present-day boundary of the North Andean Sliver in Ecuador. *Tectonics* 35, 1048-1065 (2016). https://doi.org/10.1002/2016TC004117.
 - 4. P. Lonsdale, Ecuadorian subduction system. Amer. Assoc. Pet. Geol. Bull. 62, 2454-2477 (1978).
- 5. J.-Y. Collot, E. Sanclemente, J.-M. Nocquet, A. Lepretre, A. Riboderti, P. Jarrin, et al., Subducted oceanic relief locks the shallow megathrust in central Ecuador. *J. Geophys. Res.* 122, 3286-3305 (2017). https://doi.org/10.1002/2016JB013849
- 6. J.-M. Nocquet, P. Jarrin, M. Vallée, P. A. Mothes, R. Grandin, F. Rolandone et al., Supercycle at the Ecuadorian subduction zone revealed after the 2016 Pedernales earthquake. *Nat. Geosci.* 10, 145-149 (2017). https://doi.org/10.1038/NGEO2864.
- P. A. Mothes, F. Rolandone, J.-M. Nocquet, P. A. Jarrín, A. P. Alvarado, M. C. Ruiz et al.,
 Monitoring the earthquake cycle in the northern Andes from the Ecuadorian cGPS network.
 Seism. Res. Lett. 89, 534-541 (2018). https://doi.org/10.1785/0220170243.
- 8. J. A. Kelleher, Rupture zones of large South American earthquakes and some predictions. *J. Geophys. Res.* 77, 2087-2103 (1972).
- 305
 9. K. Abe, Size of great earthquake of 1837-1979 inferred from tsunami data, *J. Geophys. Res.* 84,
 306
 1561-1568 (1979).
- 307 10. J. E. Ramirez, Earthquake history of Colombia, *Bull. Seism. Soc. Am.* 23, 13-22 (1933).
- 11. S. Migeon, C. Garibaldi, G. Ratzov, S. Schmidt, J.-Y. Collot, S. Zaragosi, L. Texier, Earthquaketriggered deposits in the subduction trench of the north Ecudaor/south Colombia margin and their implication for paleoseismology. *Mar. Geo.* 384, 47-62, (2017). https://doi.org/10.1016/j.margeo.2016.09.008.
- 12. H. Kanamori, K. C. McNally, Variable rupture mode of the subduction zone along the Ecuador-Colombia coast. *Bull. Seism. Soc. Am.* 72, 1241-1253 (1982).

- 314 13. C. Mendoza, J. W. Dewey, Seismicity associated with the great Colombia-Ecuador earthquakes
- of 1942, 1958, and 1979: Implications for barrier models of earthquake rupture. *Bull. Seism. Soc.*
- 316 *Am.* 74, 577-593 (1984).
- 317 14. S. L. Beck, L.J. Ruff, The rupture process of the great 1979 Colombia earthquake: evidence for
- 318 the asperity model. *J. Geophys. Res.* 89, 9281-9291 (1984).
- 15. L. Ye, H. Kanamori, J.-P. Avouac, L. Li, K. F. Cheung, T. Lay, The 16 April 2016, M_W 7.8 (M_S
- 320 7.5) Ecuador earthquake: A quasi-repeater of the 1942 M_S 7.5 earthquake and partial re-rupture of
- the 1906 M_S 8.6 Colombia-Ecuador earthquake. Earth Planet. Sci. Lett. 454, 248-258 (2016).
- 322 https://doi.org/10.1016/j.epsl.2016.09.006.
- 323 16. P. He, E. A. Hetland, Q. Wang, K. Ding, Y. Wen, R. Zou, Coseismic slip in the 2016 M_W 7.8
- Ecuador earthquake imaged from Sentinel-1A radar interferometry. Seism. Res. Lett. 88, 277-286
- 325 (2017). https://doi.org/10.1785/0220160151.
- 326 17. M. Heidarzadeh, S. Murotani, K. Satake, T. Takagawa, T. Saito, Fault size and depth extent of the
- Ecuador earthquake (M_W 7.8) of 16 April 2016 from teleseismic and tsunami data. *Geophys. Res.*
- 328 Lett. 44, 2211-2219 (2017). https://doi.org/10.1002/2017GL072545.
- 329 18. M. Yoshimoto, M., H. Kumagai, W. Acero, G. Ponce, F. Vásconez, S. Arrais, et al., Depth-
- dependent rupture mode along the Ecuador-Colombia subduction zone. Geophys. Res. Lett. 44,
- 331 2203-2210 (2017). https://doi.org/10.1002/2016GL071929.
- 19. J. L. Swenson, S. L. Beck, Historical 1942 Ecuador and 1942 Peru subduction earthquakes, and
- earthquake cycles along Colombia-Ecuador and Peru subduction segments. *Pure Appl. Geophys.*
- 334 146, 67-101 (1996).
- 20. H. Perfettini, J.-P. Avouac, H. Tavera, A. Kositsky, J.-M. Nocquet, F. Bondoux, et al., Seismic
- and aseismic slip on the Central Peru megathrust. *Nature* 465, 78-81 (2010).
- 337 https://doi.org/10.1038/nature09062.
- 21. J. C. Villegas-Lanza, M. Chlieh, O. Cavalié, H. Tavera, P. Baby, J. Chire-Chira, J.-M. Nocquet,
- 339 Active tectonics of Peru: Heterogeneous interseismic coupling along the Nazca megathrust, rigid
- motion of the Peruvian Sliver, and Subandean shortening accommodation. J. Geophys. Res.: Solid
- 341 Earth 121, 7371-7394 (2016). https://doi.org/10.1002/2016JB013080.
- 342 22. E. Silgado, Destructive earthquakes of South America 1530-1894, Earthquake Mitigation
- 343 Program in the Andean Region, Project SISRA, vol. 10, 315 pp., Lima, Peru (1985).
- 344 23. L. Dorbath, A. Cisternas, C. Dorbath, Assessment of the size of large and great historical
- at earthquakes in Peru. *Bull. Seism. Soc. Am.* 80, 551-576 (1990).
- 24. A. M. Pelayo, D. A. Wiens, The November 20, 1960 Peru tsunami earthquake source
- mechanism of a slow event. *Geophys. Res. Lett.* 17, 661-664 (1990).

- 25. P. F. Ihmlé, J.-M. Gomez, P. Heinrich, S. Guibourg, The 1996 Peru tsunamigenic earthquake: Broadband source process. *Geophys. Res. Lett.* 25, 2691-2694 (1998).
- 26. S. L. Bilek, Seismicity along the South American subduction zone: Review of large earthquakes, tsunamis and subduction zone complexity. *Tectonophys.* 495, 2-14 (2010).
- 352 https://doi.org/10.1016/j.tecto.2009.02.037.
- Z. Wu, T. Lay, L. Ye, Shallow megathrust slip during large earthquakes that have high P coda
 levels. J. Geophys. Res.: Solid Earth 124, e2019JB018709.
 https://doi.org/10.1029/2019JB018709.
- <u>nttps://doi.org/10.1029/2019JB018/09</u>.
- 356 28. B. L. Askew, S. T. Algermissen (eds). *Catalog of Earthquakes for South America: Hypocenter*357 *and Intensity Data* (Ceresis publication, Volumes 4, 6, and 7a, b and c) (1985).
- N. Wetzler, T. Lay, E. E. Brodsky, H. Kanamori, Rupture-depth-varying seismicity patterns for major and great (M_W ≥7.0) megathrust earthquakes. *Geophys. Res. Lett.* 44, 9663-9671 (2017). https://doi.org/10.1002/2017GL074573.
- 30. S. L. Beck, S.P. Nishenko, Variations in the mode of great earthquake rupture along the central Peru subduction zone. *Geophys. Res. Lett.* 17, 1969-1972 (1990).
- 31. J. W. Dewey, W. Spence, Seismic gaps and source zones of recent large earthquakes in coastal Peru. *Pure Appl. Geophys.*, 117, 1148-1171 (1979).
- 32. S. L. Beck, L.J. Ruff, Great earthquakes and subduction along the Peru trench. *Phys. Earth Planet. Int.* 57, 199-224 (1989).
- 33. C. J. Langer, W. Spence, The 1974 Peru earthquake series. *Bull. Seism. Soc. Am.* 85, 665-687 (1995).
- 34. T. Lay, C. J. Ammon, A. R. Hutko, H. Kanamori, Effects of kinematic constraints on teleseismic finite-source rupture inversions: Great Peruvian earthquakes of 23 June 2001 and 15 August 2007. *Bull. Seism. Soc. Am.* 100, 969-994 (2010). https://doi.org/10.1785/0120090274.
- 35. A. Sladen, H. Tavera, M. Simons, J. P. Avouac, A. O. Konca, H. Perfettini, L. Audin, E. J.
- Fielding, F. Ortega, R. Cavagnoud, Source model of the 2007 M_w 8.0 Pisco, Peru earthquake:
- Implications for seismogenic behavior of subduction megathrusts. *J. Geophys. Res.* 115, B02405
- 375 (2010). https://doi.org/10.1029/2009JB006429.
- 36. M. Chlieh, H. Perfettini, H. Tavera, J.-P. Avouac, D. Remy, J.-M. Nocquet et al., Interseismic coupling and seismic potential along the Central Andes subduction zone. *J. Geophys. Res.* 116, B12405 (2011). https://doi.org/10.1029/2010JB008166.
- 37. M. E. Pritchard, E. O. Norabuena, C. Ji, R. Boroschek, D. Comte, M. Simons, T. H. Dixon, P. A.
 380 Rosen, Geodetic, teleseismic, and strong motion constraints on slip from recent southern Peru

- 381 subduction zone earthquakes. *J. Geophys. Res.* 112, B03307 (2007).
 382 https://doi.org/10.1029/2006JB004294.
- 38. M. Motagh, R. Wang, T. R. Walter, R. Bürgmann, E. Fielding, J. Anderssohn, J. Zschau, Coseismic slip model of the 2007 August Pisco earthquake (Peru) as constrained by wide swath radar observations. *Geophys. J. Int.* 174, 842-848 (2008).
- 39. M. E. Pritchard, E. J. Fielding, A study of the 2006 and 2007 earthquake sequence of Pisco, Peru, 386 387 with InSAR and teleseismic data. Geophys. Res. Lett. 35, L09308 (2008).https://doi.org/10.1029/2008GL033374. 388
- 40. H. Tavera, I. Bernal, The Pisco (Peru) earthquake of 15 August 2007. Seismol. Res. Lett. 79, 510 515 (2008). https://doi.org/10.1785/gssrl.79.4.510.
- 391 41. J. D. Biggs, P. Robinson, T. H. Dixon, The 2007 Pisco, Peru, earthquake (*M* 8.0): seismology and
 392 geodesy. *Geophys. J. Int.* 176, 657-669 (2009).
 393 https://doi.org/10.1111/j.1365-246X.2008.03990.x.
- 394 42. O. Sufri, K. D. Koper, T. Lay, Along-dip seismic radiation segmentation during the 2007 M_W 8.0 395 Pisco, Peru earthquake. *Geophys. Res. Lett.* 39, L08311 (2012). 396 https://doi.org/10.1029/2012GL051316.
- 43. M. Ioualalen, H. Perettini, S. Yauri Condo, C. Jimenez, H. Tavera, Tsunami modeling to validate
 slip models of the 2007 M_W 8.0 Pisco earthquake, Central Peru. Pure Appl. Geophys. 170, 433 451 (2013). https://doi.org/10.1007/s00024-012-0608-z.
- 40. D. Comte, M. Pardo, Reappraisal of great historical earthquakes in the Northern Chile and Southern Peru seismic gaps. *Nat. Haz.* 4, 23-44 (1991).
- 402 45. J. L. Swenson, S. L. Beck, Source characteristics of the 12 November 1996 M_W 7.7 Peru subduction zone earthquake. *Pure Appl. Geophys.* 154, 731-751 (1999).
- 46. M. K. Giovanni, S. L. Beck, L. Wagner (2002), The June 23, 2001 Peru earthquake and the southern Peru subduction zone. *Geophys. Res. Lett.* 29, 2018 (2002).
 https://doi.org/10.1029/2002GL015774.
- 407 47. S. L. Bilek, L. J. Ruff, Analysis of the 23 June 2001 M_W = 8.4 Peru underthrusting earthquake and 408 its aftershocks. *Geophys. Res. Lett.* 29, 1960 (2002). https://doi.org/10.1029/2002GL015543.
- 48. D. P. Robinson, S. Das, A. B. Watts, Earthquake rupture stalled by a subducting fracture zone.

 Science 312, 1203-1205 (2006). https://doi.org/10.1126/science.1125771.
- 49. C. Jiménez, C. Carbonel, J. C. Villegas-Lanza, Seismic source of the earthquake of Camana Peru
 2001 (M_W 8.2) from joint inversion of geodetic and tsunami data. *Pure Appl. Geophys.* 178, 4763-413
 4775 (2021). https://doi.org/10.1007/s00024-020-02616-8.

- 414 50. H. Perfettini, J.-P. Avouac, J. Ruegg, Geodetic displacements and aftershocks following the 2001,
- 415 $M_W = 8.4$ Peru earthquake: implications for the mechanics of the earthquake cycle along
- subduction zones. *J. Geophys. Res.* 110, B09404 (2005). https://doi.org/10.1029/2004JB003522.
- 417 51. J. P. Loveless, M. E. Pritchard, N. Kukowski, Testing mechanisms of subduction zone
- 418 segmentation and seismogenesis with slip distributions from recent Andean earthquakes.
- 419 Tectonophys. 495, 15-33 (2010). https://doi.org/10.1016/j.tecto.2009.05.008.
- 420 52. S. Ruiz, R. Madariaga, Historical and recent large megathrust earthquakes in Chile. *Tectonophys*.
- 421 733, 37-56 (2018). https://doi.org/10.1016/j.tecto.2018.01.015.
- 422 53. G. Vargas, L. Ortlieb, E Chapron, J. Valdes, C. Marquardt, Paleoseismic inerences from a high-
- resolution marine sedimentary record in northern Chile (23°S). *Tectonophys.* 399 381-398 (2005).
- 424 https://doi.org/10.1016/j.tecto.2004.12.031.
- 425 54. M. Abad, T. Izquierdo, M. Cáceres, E. Bernández, J. Rodríguez-Vidal, Coastal boulder deposit as
- evidence of an ocean-wide prehistoric tsunami originated on the Atacama Desert coast (northern
- 427 Chile). Sedimentology 67, 1505-1528 (2020).
- 428 55. I. Tsuji, Catalog of distant tsunamis researching Japan from Chile and Perú. Rep. Tsunami Eng.
- 429 30, 61-68 (2013).
- 430 56. D. Salazar, G. Easton, J. Goff, J. L. Guendon, J. González-Alfaro, P. Andrade, et al., Did a 3800-
- 431 year-old $M_W \sim 9.5$ earthquake trigger major social disruption in the Atacama desert? Sci. Adv. 8,
- eabm2996 (2022). https://doi.org/10.1126/sciadv.abm2996.
- 57. C. An, I. Sepúlveda, P. L.-F. Liu, Tsunami source and its validation of the 2014 Iquique, Chile,
- 434 earthquake. Geophys. Res. Lett., 41 3988-3994 (2014). https://doi.org/10.1002/2014GL060567.
- 58. G. P. Hayes, M. W. Herman, W. D. Barnhart, K. P. Furlong, S. Riquelme, H. M. Benz, et al.,
- Continuing megathrust earthquake potential in Chile after the 2014 Iquique earthquake. *Nature*
- 437 512, 295-298 (2014). https://doi.org/10.1038/nature13677.
- 438 59. T. Lay, H. Yue, E. E. Brodsky, C. An, The 1 April 2014 Iquique, Chile M_W 8.1 earthquake
- 439 rupture sequence. *Geophys. Res. Lett.* 41, 3818-3825 (2014).
- https://doi.org/10.1002/2014GL060238.
- 441 60. Y. Bai, K. F. Cheung, Y. Yamazaki, T. Lay, L. Ye, Tsunami surges around the Hawaiian Islands
- from the 1 April 2014 North Chile M_W 8.1 earthquake. Geophys. Res. Lett. 41, 8512-8521 (2014).
- https://doi.org/10.1002/2014GL061686.
- 444 61. Y. Yagi, R. Okuwaki, B. Enescu, S. Hirano, Y. Yamagami, S. Endo, T. Komoro, Rupture process
- of the 2014 Iquique Chile Earthquake in relation with the foreshock activity. *Geophys. Res. Lett.*
- 446 41, 4201-4206 (2014). https://doi.org/10.1002/2014GL060274.

- 447 62. A. R. Gusman, S. Murotani, K. Satake, M. Heidarzadeh, E. Gunawan, S. Watada, B. Schurr, Fault 448 slip distribution of the 2014 Iquique, Chile earthquake estimated from ocean-wide tsunami waveforms 42. 1053-1060 449 and GPS data. Geophys. Res. Lett. (2015).https://doi.org/10.1002/2014GL062604. 450
- 451 63. Z. Duputel, J. Jiang, R. Jolivet, M. Simons, L. Rivera, J.-P. Ampuero, et al., The Iquique earthquake sequence of April 2014: Bayesian modeling accounting for prediction uncertainty.

 453 Geophys. Res. Lett. 42, 7949-7957 (2015). https://doi.org/10.1002/2015GL065402.
- 64. C. Liu, Y. Zheng, R. Wang, X. Xiong, Kinematic rupture process of the 2014 Chile M_W 8.1
 earthquake constrained by strong-motion, GPS static offsets and teleseismic data. *Geophys. J. Int.* 202, 1137-1145 (2015). https://doi.org/10.1093/gji/ggv214.
- 457 65. E. E. Brodsky, T. Lay, Recognizing foreshocks from the 1 April 2014 Chile earthquake, *Science* 344, 700-702 (2014). https://doi.org/10.1126/science.1255202.
- 459 66. A. Kato, S. Nakagawa, Multiple slow-slip events during a foreshock sequence of the 2014
 460 Iquique, Chile M_W 8.1 earthquake. Geophys. Res. Lett. 41, 5420-5427 (2014).
 461 https://doi.org/10.1002/2014GL061138.
- 462 67. S. Ruiz, M. Métois, A. Fuenzalida, J. Ruiz, F. Leyton, R. Grandin, C. Vigny, R. Madariaga, J.
 463 Campos, Intense foreshocks and a slow slip event preceded the 2014 Iquique M_W 8.1 earthquake.
 464 Science 345, 1165-1169 (2014). https://doi.org/10.1126/science.1256074.
- 465 68. B. Schurr, G. Asch, S. Hainzl, J. Bedford, A. Hoechner, M. Palo, et al., Gradual unlocking of
 466 plate boundary controlled initiation of the 2014 Iquique earthquake. *Nature* 512, 299-302 (2014).
 467 https://doi.org/10.1038/nature13681.
- 468 69. L. Meng, H. Huang, R. Bürgmann, J. P. Ampuero, A. Strader, Dual megathrust slip behaviors of
 469 the 2014 Iquique earthquake sequence. *Earth Plant. Sci. Lett.* 411, 177-187 (2015).
 470 https://doi.org/10.1016/j.epsl.2014.11.041.
- 70. S. Cesca, F. Grigoli, S. Heimann, T. Dahmn, M. Kriegerowski, M. Sobiesisak, et al., The M_W 8.1
 2014 Iquique, Chile, seismic sequence: a tale of foreshocks and aftershocks. *Geophys. J. Int.* 204,
 1766-1780 (2016). https://doi.org/10.1093/gji/ggv544.
- 71. A. Socquet, J. P. Valdes, J. Jara, F. Cotton, A. Walpersdorf, N. Cotte, et al., An 8 months slow slip event triggers progressive nucleation of the 2014 Chile megathrust. *Geophys. Res. Lett.* 44, 476 4046-4053 (2017). https://doi.org/10.1002/2017GL073023.
- 72. F. Hoffmann, S. Metzger, M. Moreno, Z. Deng, C. Sippl, F. Ortega-Culaciati, O. Oncken, Characterizing afterslip and ground displacement rate increase following the 2014 Iquique-Pisagua M_W 8.1 earthquake, Northern Chile. *J. Geophys. Res.: Solid Earth* 123, 4171-4192 (2018). https://doi.org/10.1002/2017JB014970.

- 481 73. M. Chlieh, J. B. de Chabalier, J. C. Ruegg, R. Armijo, R. Dmowska, J. Campos, K. L. Feigl,
- Crustal deformation and fault slip during the seismic cycle in the North Chile subduction zone,
- from GPS and InSAR observations. Geophys. J. Int. 158, 695-711 (2004).
- 484 https://doi.org/10.1111/j.1365-246X.2004.02326.x.
- 485 74. M. Métois, A. Socquet, C. Vigny, D. Carrizo, S. Peyrat, A. Delorme, et al., Revisiting the North
- Chile seismic gap segmentation using GPS-derived interseismic coupling. *Geophys. J. Int.* 194,
- 487 1283-1294 (2013). https://doi.org/10.1093/gji/ggt183.
- 488 75. E. Kausel, Los terremotos de Agosto de 1868 y Mayo de 1877 que afectaron el sur del Perú y
- 489 norte de Chile. *Boletín de la Academia Chilena de Ciencias* 3, 8-13 (1986).
- 490 76. C. Vigny, E. Klein, The 1877 megathrust earthquake of North Chile two times smaller than
- thought? A review of ancient articles. J. S. Amer. Earth Sci. 117, 103878 (2022).
- 492 https://doi.org/10.1016/j.jsames.2022.103878.
- 493 77. Delouis, B., M. Pardo, D. Legrand, T. Monfret, The M_W 7.7 Tocopilla earthquake of 14
- November 2007 at the southern edge of the northern Chile seismic gap: Rupture in the deep part
- of the coupled plate interface. Bull. Seism. Soc. Am. 99, 87-94 (2009).
- 496 https://doi.org/10.1785/0120080192.
- 497 78. M. Béjar-Pizarro, Asperities and barriers on the seismogenic zone in North Chile: state-of-the-art
- 498 after the 2007 M_W 7.7 Tocopilla earthquake inferred by GPS and InSAR data. Geohys. J. Int. 183,
- 499 390-406 (2010). https://doi.org/10.1111/j.1365-246X.2010.04748.x
- 500 79. S. Peyrat, R. Madariaga, E. Buforn, J. Campos, G. Asch, J. P. Vilotte, Kinematic rupture process
- of the 2007 Tocopilla earthquake and its main aftershocks from teleseismic and strong motion
- 502 data. Geophys. J. Int, 182, 1411-1430 (2010).
- 503 https://doi.org/10.1111/j.1365-246X.2010.04685.x.
- 80. B. Schurr, G. Asch, M. Rosenau, R. Wang, O. Oncken, S. Barrientos, P. Salazar, J.-P. Vilotte,
- The 2007 M7.7 Tocopilla northern Chile earthquake sequence: Implications for along-strike and
- downdip rupture segmentation and megathrust frictional behavior. J. Geophys. Res. 117, B05305
- 507 (2012). https://doi.org/10.1029/2011JB009030.
- 508 81. J. C. Ruegg, J. Campos, R. Armijo, S. Barrientos, P. Briole, R. Thiele, et al., The M_W =8.1
- Antofagasta (North Chile) earthquake of July 30, 1995: First results from teleseismic and
- geodetic data. *Geophys. Res. Lett.* 23, 917-920 (1996).
- 511 82. Delouis, B., T. Monfret, L. Dorbath, M. Pardo, L. Rivera, D. Comte, et al., The $M_W = 8.0$
- Antofagasta (Northern Chile) earthquake of 30 July 1995: A precursor to the end of the larger
- 513 1877 gap. Bull. Seism. Soc. Am. 87, 427-445 (1997).

- 83. P. F. Ihmlé, J.-C. Ruegg, Source tomography by simulated annealing using broad-band surface
- waves and geodetic data: application to the M_W =8.1 Chile 1995 event. Geophys. J. Int. 131, 146-
- 516 158 (1997).
- 517 84. S. Guibourg, P. Heinrich, R. Roche, Numerical modeling of the 1995 Chilean tsunami. Impact on
- French Polynesia. *Geophys. Res. Lett.* 24, 775-778 (1997).
- 85. D. L. Carlo, T. Lay, C. J. Ammon, J. Zhang, Rupture process of the 1995 Antofagasta subduction
- 520 earthquake ($M_W = 8.1$). Pure Appl. Geophys. 154 677-709 (1999).
- 521 86. J. Klotz, D. Angermann, G. W. Michel, R. Porth, C. Reigber, J. Reinking, et al., GPS-derived
- deformation of the central Andes including the 1995 Antofagasta $M_W = 8.0$ earthquake. Pure
- 523 Appl. Geophys. 154 709-730 (1999).
- 87. M. E. Pritchard, M. Simons, P. A. Rosen, S. Hensley, F. H. Webb, Co-seismic slip rom the 1995
- July 30 M_W =8.1 Antofagasta, Chile, earthquake as constrained by InSAR and GPS observations.
- 526 Geophys. J. Int. 150, 362-376 (2002).
- 88. M. E. Pritchard, C. Ji, M. Simons, Distribution of slip from 11 $M_W > 6$ earthquake in the northern
- 528 Chile subduction zone, J. Geophys. Res. 111, B10302 (2006).
- 529 https://doi.org/10.1029/2005JB004013.
- 89. M.E. Pritchard, M. Simons, An aseismic slip pulse in northern Chile and along-strike variations
- in seismogenic behavior. J. Geophys. Res. 111, B08405 (2006).
- 532 https://doi.org/10.1029/2006JB004258.
- 90. P. F. Ihmlé, R. Madariaga, Monochromatic body waves excited by great subduction zone
- earthquakes. *Geophys. Res. Lett.* 23, 2999-3002 (1996).
- 535 91. S. Beck, S. Barrientos, E. Kausel, M. Reyes, Source characteristics of historic earthquakes along
- the central Chile subduction zone. J. South Am. Earth Sci. 11, 115–129 (1998).
- 537 92. C. Lomnitz, C., Major earthquakes of Chile: A historical survey, 1535 1960. Seism. Res. Lett.
- 538 75, 368-378 (2004). https://doi.org/10.1785/gssrl.75.3.368.
- 93. H. Kanamori, L. Rivera, L. Ye, T. Lay, S. Murotani, K. Tsumura, New constraints on the 1922
- Atacama, Chile, earthquake from historical seismograms. *Geophys. J. Int.* 219, 645-661 (2019).
- 541 https://doi.org/10.1093/gji/ggz302.
- 542 94. G. Easton, J. González-Alfaro, A. Villalobos, G. Álvarez, D. Melgar, S. Ruiz, B. Sepúlveda, M.
- Escobar, T. León, J. Carlos Báez, et al., Complex rupture of the 2015 M_W 8.3 Illapel earthquake
- and prehistoric events in the Central Chile tsunami gap. Seis. Res. Lett. 93, 1479–1496 (2022).
- 545 https://doi.org/10.1785/0220210283.

- 95. M. Métois, A. Socquet, C. Vigny, Interseismic coupling, segmentation and mechanical behavior of the central Chile subduction zone. *J. Geophys. Res.* 117, B03406 (2012). https://doi.org/10.1029/2011JB008736.
- M. Métois, C. Vigny, A. Socquet, A. Delorme, S. Morvan, I. Ortega, C. M. Valderas-Bermejo,
 GPS-derived interseismic coupling on the subduction and seismic hazards in the Atacama region,
 Chile, *Geophys. J. Inter.*, 196, 644-655 (2014). https://doi.org/10.1093/gji/ggt418.
- M. W. Herman, R. Govers, Locating fully locked asperities along the South America subduction
 megathrust: A new physical inter-seismic inversion approach in a Bayesian framework.
 Geochem. Geophys., Geosys. 21, e2020GC009063 (2020).
- 555 98. C. Lomnitz, Major earthquakes and tsunamis in Chile during the period 1535 to 1953. *Geol. Rundsch.* 59, 938-960 (1970).
- 557 99. S. P. Nishenko, Seismic potential for large and great interplate earthquakes along the Chilean and southern Peruvian margins of South America: A quantitative reappraisal. *J. Geophys. Res.* 90, 3589–3615 (1985). https://doi.org/10.1029/JB090iB05p03589.
- L. Ye, T. Lay, H. Kanamori, K.D. Koper, Rapidly estimated seismic source parameters for the 16
 September 2015 Illapel Chile M_W 8.3 earthquake. Pure Appl. Geophys. 173, 321-332 (2016).
 https://doi.org/10.1007/s00024-015-1202-y.
- 563 101. M. Heidarzadeh, S. Murotani, K. Satake, T. Ishibe, A. R. Gusman, Source model of the 16 564 September 2015 Illapel, Chile M_W 8.4 earthquake based on teleseismic and tsunami data. 565 *Geophys. Res. Lett.* 43, 643-650 (2016). https://doi.org/10.1002/2015GL067297.
- L. Li, T. Lay, K. F. Cheung, L. Ye, Joint modeling of teleseismic and tsunami wave observations
 to constrain the 16 September 2015 Illapel, Chile, M_W 8.3 earthquake rupture process. *Geophys. Res. Lett.* 43, 4303-4312 (2016). https://doi.org/10.1002/2016GL068674.
- 103. D. Melgar, W. Fan, S. Riquelme, J. Geng, C. Liang, M. Fuentes, G. Vargas, R. M. Allen, P. M. 569 570 Shearer, E. J. Fielding, Slip segmentation and slow rupture to the trench during the 2015, $M_W 8.3$ 571 Illapel, Chile earthquake. Geophys. Res. Lett. 43. 961-966 (2016).572 https://doi.org/10.1002/2015GL067369.
- 104. R. Okuwaki, Y. Yagi, R. Aránguiz, J. González, G. González, Rupture process during the 2015
 Illapel, Chile Earthquake: Zigzag-along-dip rupture episodes. *Pure. Appl. Geophys.* 173, 1011 1020 (2016). https://doi.org/10.1007/s00024-016-1271-6.
- 576 105. S. Ruiz, E. Klein, F. del Campo, E. Rivera, P. Poli, M. Metois, V. Christophe, J.C. Baez, G. 577 Vargas, F. Leyton, R. Madariaga, L. Fleitout, The seismic sequence of the 16 September 2015 578 8.3 Illapel, Chile earthquake. Seism. Res. Lett. 87, 789-799 (2016).579 https://doi.org/10.1785/0220150281.

- 106. F. Tilmann, Y. Zhang, M. Moreno, J. Saul, F. Eckelmann, M. Palo et al., The 2015 Illapel earthquake, central Chile: A type case for a characteristic earthquake? *Geophys. Res. Lett.* 43, 574–583 (2016). https://doi.org/10.1002/2015GL066963.
- 583 107. J. Yin, H. Yang, H. Yao, H. Weng, Coseismic radiation and stress drop during the 2015 M_W 8.3 Illapel, Chile megathrust earthquake. *Geophys. Res. Lett.* 43, 1520-1528 (2016). https://doi.org/10.1002/2015GL067381.
- 586 108. C. An, H. Yue, J. Sun, L. Meng, J. C. Báez, The 2015 M_W 8.3 Illapel, Chile, earthquake:
 587 Direction-reversed along-dip rupture with localized water reverberation. *Bull. Seism. Soc. Am.*,
 588 107, 2416-2426 (2017). https://doi.org/10.1785/0120160393.
- M. W. Herman, J. L. Nealy, W. L. Yeck, W. D. Barnhart, G. P. Hayes, K. P. Furlong, H. M.
 Benz, Integrated geophysical characteristics of the 2015 Illapel, Chile, earthquake. *J. Geophys. Res.: Solid Earth* 122, 4691-4711 (2017). https://doi.org/10.1002/2016JB013617.
- 110. E. Klein, C. Vigny, L. Fleitout, R. Grandin, R. Jolivet, E. Rivera, M. Métois, A comprehensive
 analysis of the Illapel 2015 M_W 8.3 earthquake from GPS and InSAR data. *Earth Planet. Sci. Lett.* 469, 123-134 (2017). https://doi.org/10.1016/j.epsl.2017.04.010.
- 111. K. Satake, M. Heidarzadeh, A review of source models of the 2015 Illapel, Chile earthquake and insights from tsunami data. *Pure Appl. Geophys.* 174, 1-9 (2017).
 https://doi.org/10.1007/s00024-016-1450-5.
- A. Williamson, A. Newman, and P. Cummins, Reconstruction of coseismic slip from the 2015
 Illapel earthquake using combined geodetic and tsunami waveform data/ *J. Geophys. Res. Solid Earth* 122, 2119-2130 (2017). https://doi.org/10.1002/2016JB013883.
- 113. C. Liu, C. An, B. Shan, X. Xiong, X. Chen, Insights into the kinematic rupture of the 2015 M_W
 8.3 Illapel, Chile, earthquake from joint analysis of geodetic, seismological, tsunami, and superconductive gravimeter observations. *J. Geophys. Res.: Solid Earth* 123, 9778-7999 (2018).
 https://doi.org/10.1029/2018JB016065.
- 114. C. Vigny, A. Rudloff, J.-C. Ruegg, R. Madariaga, J. Campos, M. Alvarez, Upper plate deformation measured by GPS in the Coquimbo Gap, Chile. *Phys. Earth Planet. Inter.* 175, 86–95 (2009). https://doi.org/10.1016/j.pepi.2008.02.013.
- M. Métois, C. Vigny, A. Socquet, Interseismic coupling, megathrust earthquakes and seismic swarms along the Chilean subduction zone (38°-18°S). *Pure Appl. Geophys.* 1783, 1431-1449 (2016).
- 611 116. M. N. Shrivastava, G. González, M. Moreno, M. Chlieh, P. Salazar, C. D. Reddy, et al., 612 Coseismic slip and afterslip of the 2015 M_W 8.3 Illapel (Chile) earthquake determined from

- 613 continuous GPS data. *Geophys. Res. Lett.* 43, 10710-10719 (2016). 614 https://doi.org/10.1002/2016GL070684.
- 117. W. Feng, S. Samsonov, Y. Tian, Q. Qiu, P. Li, Y. Zhang, Z. Deng, K. Omari, Surface deformation associated with the 2015 M_W 8.3 Illapel earthquake revealed by satellite-based geodetic observations and its implications for the seismic cycle. *Earth Planet. Sci. Lett.* 460,
- 618 222-233 (2017). https://doi.org/10.1016/j.epsl.2016.11.018.
- 118. H. Huang, W. Xu, L. Meng, R. Burgmann, J. C. Baez, Early aftershocks and afterslip surrounding the 2015 M_W 8.4 Illapel rupture. *Earth Planet Sci. Lett.* 457, 282-291 (2017). https://doi.org/10.1016/j.epsl.2016.09.055.
- 119. R. Aránguiz, G. González, J. González, P. A. Catalán, R. Cienfuegos, Y. Yagi, et al., The 16
 September 2015 Chile tsunami from the post-tsunami survey and numerical modeling
 perspectives, *Pure Appl. Geophys.* 333-348 (2016). https://doi.org/10.1007/s00024-015-1225-4.
- 120. M. Contreras-López, P. Winckler, I. Sepúlveda, A. Anduar-Álvarez, F. Cortés-Molina, C. J.
 Gueerrero, et al., Field survey of the 2015 Chile tsunami with emphasis on coastal wetland and
 conservation areas. *Pure Appl. Geophys.* 173, 349-367 (2016).
 https://doi.org/10.1007/s00024-015-1235-2.
- B. Delouis, J.-M. Nocquet, M. Vallée, Slip distribution of the February 27, 2010 M_W = 8.8 Maule
 earthquake, central Chile, from static and high-rate GPS, InSAR and broadband teleseismic data.
 Geophys. Res. Lett. 37, L17305 (2010). https://doi.org/10.1029/2010GL043899.
- 122. T. Lay, C. J. Ammon, H. Kanamori, K. D. Koper, O. Sufri, A. R. Hutko, Teleseismic inversion
 for rupture process of the 27 February 2010 Chile (M_W 8.8) earthquake. Geophys. Res. Lett. 37,
 L11301 (2010). https://doi.org/10.1029/2010GL043379.
- 123. M. Moreno, M. Rosenau, O. Oncken, 2010 Maule earthquake slip correlates with pre-seismic locking of Andean subduction zone. *Nature* 467, 198–202 (2010).
 https://doi.org/10.1038/nature09349.
- 124. X. Tong, D. Sandwell, K. Luttrell, B. Brooks, M. Bevis, M. Shimada, et al., The 2010 Maule, Chile earthquake: Downdip rupture limit revealed by space geodesy. *Geophys. Res. Lett.* 37, L24311 (2010). https://doi.org/10.1029/2010GL045805.
- 125. F. Pollitz, B. Brooks, X. Tong, M. G. Bevis, J. H. Foster, R. Bürgmann, et al., Coseismic slip distribution of the February 27, 2010 M_W 8.8 Maule, Chile earthquake. *Geophys. Res. Lett.* 38, L09309 (2011). https://doi.org/10.1029/2011GL047065.
- 126. C. Vigny, A. Socquet, S. Peyrat, J.-C. Ruegg, M. Métois, R. Madariaga, et al., The 2010 M_W 8.8 Maule mega-thrust earthquake of central Chile, monitored by GPS. *Science* 332, 1417-1421 (2011). https://doi.org/10.1126/science.1204132.

- 647 127. Y. Fujii, K. Satake, Slip distribution and seismic moment of the 2010 and 1960 Chilean 648 earthquakes inferred from tsunami waveforms and coastal geodetic data. *Pure Appl. Geophys*. 649 170, 1493-1509 (2013). https://doi.org/10.1007/s00024-012-0524-2.
- K. D. Koper, A. R. Hutko, T. Lay, O. Sufri, Imaging short-period seismic radiation from the 27
 February 2010 Chile (M_W 8.8) earthquake by back-projection of P, PP, and PKIKP waves. J.
 Geophys. Res: Solid Earth 117, B02308 (2012). https://doi.org/10.1029/2011JB008576.
- M. Moreno, D. Melnick, M. Rosenau, J. Baez, J. Klotz, O. Oncken, et al., Toward understanding
 tectonic control on the M_W 8.8 2010 Maule Chile earthquake. *Earth Planet. Sci. Lett.* 321-322,
 152-165 (2012). https://doi.org/10.1016/j.epsl.2012.01.006.
- 130. G. P. Hayes, E. Bergman, K. L Johnson, H. M. Benz, L. Brown, A. S. Meltzer, Seismotectonic framework of the 2010 February 27 M_W 8.8 Maule, Chile earthquake sequence. *Geophys. J. Int.* 195, 1034-1051 (2013). https://doi.org/10.1093/gji/ggt238.
- 131. Y. N. Lin, A. Sladen, F. Ortega-Culaciati, M. Simons, J.-P. Avouac, E. J. Fielding, et al.,
 Coseismic and postseismic slip associated with the 2010 Maule earthquake, Chile: characterizing
 the Arauco Peninsula barrier effect. *J. Geophys. Res.: Solid Earth* 118, 3142-3159 (2013).

 https://doi.org/10.1002/jgrb.50207.
- H, Yue, T. Lay, L. Rivera, C. An, C. Vigny, X. Tong, J. C. Báez Soto, Localized fault slip to the
 trench in the 2010 Maule, Chile M_w 8.8 earthquake from joint inversion of high-rate GPS,
 teleseismic body waves, InSAR, campaign GPS, and tsunami observations. *J. Geophys. Res.* 119,
 7786-7804 (2014). https://doi.org/10.1002/2014JB011340.
- 667 133. M. Yoshimoto, S. Watada, Y. Fujii, K. Satake, Source estimate and tsunami forecast from far-668 field deep-ocean tsunami waveforms – The 27 February 2010 M_W 8.8 Maule earthquake. 669 *Geophys. Res. Lett.* 43, 659-665 (2016). https://doi.org/10.1002/2015GL067181.
- 134. F. Romano, S. Lorito, T. Lay, A. Piatanesi, M. Volpe, S. Murphy, R. Tonini, Benchmarking the 670 optimal time alignment of tsunami waveforms in nonlinear joint inversions for the M_W 8.8 2010 671 585429 8, (2020).672 Maule (Chile) earthquake. Frontiers inEarth Science 673 https://doi.org/10.3389/feart.2020.585429.
- A. Maksymowicz, C. D. Chadwell, J. Ruiz, A. M. Tréhu, E. Contreras-Reyes, W. Weinrebe, et
 al., Coseismic seafloor deformation in the trench region during the M_W 8.8 Maule megthrust
 earthquake. Sci. Rep., 7, 45918 (2017). https://doi.org/10.1038/srep45918.
- 136. A. Rietbrock, I. Ryder, G. Hayes, C. Haberland, D. Comte, S. Roecker, H. Lyon-Caen,
 Aftershock seismicity of the 2010 Maule $M_W = 8.8$, Chile, earthquake: Correlation between coseismic slip models and aftershock distribution? *Geophys. Res. Lett.* 39, L08310 (2012).
 https://doi.org/10.1029/2012GL051308.

- 137. J. C. Ruegg, J. C., A. Rudloff, C. Vigny, R. Madariaga, J. B. de Chabalier, J. Campos, E. Kausel,
- S. Barrientos, D. Dimitrov, Interseismic strain accumulation measured by GPS in the seismic gap
- between Constitución and Concepción in Chile. Phys. Earth Planet Inter. 175, 78-85 (2009).
- https://doi.org/10.1016/j.pepi.2008.02.015.
- 685 138. S. Lorito, F. Romano, S. Atzori, X. Tong, A. Avallone, J. McCloskey, et al., Limited overlap
- between the seismic gap and coseismic slip of the great 2010 Chile earthquake. Nature
- Geoscience 4, 173-177 (2011). https://doi.org/10.1038/ngeo1073.
- 688 139. J. Bedford, M. Moreno, J. C. Baez, D. Lange, F. Tilmann, M. Rosenau, C. Vigny, A high-
- resolution, time-variable afterslip model for the 2010 Maule $M_W = 8.8$, Chile megathrust
- 690 earthquake. *Earth Planet. Sci. Lett.* 383, 26–36 (2013).
- https://doi.org/10.1016/j.epsl.2013.09.020.
- 692 140. E. Klein, L. Fleitout, C. Vigny, J. D. Garaud, Afterslip and viscoelastic relaxation model inferred
- rom the large-scale post-seismic deformation following the 2010 M_W 8.8 Maule earthquake
- 694 (Chile). *Geophys. J. Int.* 205, 1455-1472 (2016). https://doi.org/10.1093/gji/ggw086.
- 695 141. D. Comte, A. Eisenberg, E. Lorac, M. Pardo, L. Ponce, R. Saragoni, S. K. Singh, G. Suarez, The
- 696 1985 central Chile earthquake: A repeat of previous great earthquakes in the region? *Science* 233,
- 697 449–453 (1986).
- 698 142. M. Cisternas, B. F. Atwater, F. Rorrejón, Y. Sawai, G. Machuca, M. Lagos, A. Eipert, C.
- Youlton, I. Salgado, T. Kamataki, et al., Predecessors of the giant 1960 Chile earthquake. *Nature*
- 700 437, 404-407 (2005).
- 701 143. M. Cisternas, M. Carvajal, R. Wesson, L. L. Ely, N. Gorigoitia, Exploring the historical
- 702 earthquakes preceding the giant 1960 Chile earthquake in a time-dependent seismogenic zone.
- 703 Bull. Seism. Soc. Am. 107, 2664-2675 (2017). https://doi.org/10.1785/0120170103.
- 144. G. Plafker, J. Savage, Mechanism of the Chilean earthquake of May 21 and 22, 1960. *Geol. Soc.*
- 705 *Am. Bull.* 81, 1001-1030 (1970).
- 706 145. G. Plafker, Alaskan earthquake of 1964 and Chilean earthquake of 1960: Implications for arc
- 707 tectonics. J. Geophys. Res. 77, 901-925 (1972).
- 708 146. H. Kanamori, J. Cipar, Focal process of the great Chilean earthquake May 22, 1960. Phys. Earth
- 709 *Planet Inter.* 9, 128-136 (1974).
- 710 147. I. L. Cifuentes, P. G. Silver, Low-frequency source characteristics of the great 1960 Chilean
- 711 earthquake. *J. Geophys. Res.* 94, 643-663 (1989).
- 712 148. S. Barrientos, S. Ward, The 1960 Chile earthquake: Inversion for slip distribution from surface
- 713 deformation. *Geophys. J. Int.* 103, 589-598 (1990).

- 149. M. S. Moreno, J. Bolte, J. Klotz, D. Melnick, Impact of megathrust geometry on inversion of coseismic slip from geodetic data: application to the 1960 Chile earthquake. *Geophys. Res. Lett.* 36, L16310 (2009). https://doi.org/10.1029/2009GL039276.
- 150. H. Kanamori, L. Rivera, S. Lambotte, Evidence for a large strike-slip component during the 1960
 Chilean earthquake. Geophys. J. Int., 218, 1-32 (2019). https://doi.org/10.1093/gji/ggz113.
- 151. E. Garrett, I. Shennan, S. A. Woodroe, M. Cisternas, E. P. Hocking, P. Gulliver, Reconstructing paleoseismic deformation, 2: 1000 years of great earthquakes at Chucalén, south central Chile.
 721 *Quat. Sci. Rev.* 113, 112-122 (2015). https://doi.org/10.1016/j.quascirev.2014.10.010.
- T. Dura, B. P. Horton, M. Cisternas, L. L. Ely, I Hong, A. R. Nelson, et al., Subduction zone slip variability during the last millennium, south –central Chile. *Quat. Sci. Rev* 175, 112-137 (2017).
 https://doi.org/10.1016/j.quascirev.2017.08.023.